

6-2019

Protective Effects of Novel Derivatives of Vitamin D₃ and Lumisterol Against UVB-Induced Damage in Human Keratinocytes Involve Activation of Nrf2 and p53 Defense Mechanisms


Anyamanee Chaiprasongsuk
The University of Alabama at Birmingham

Zorica Janjetovic
The University of Alabama at Birmingham

Tae-Kang Kim
The University of Alabama at Birmingham

Stuart G. Jarrett
University of Kentucky, stuart.jarrett@uky.edu

John A. D'Orazio
University of Kentucky, jdorazio@uky.edu
Follow this and additional works at: https://uknowledge.uky.edu/toxicology_facpub

 Part of the [Biology Commons](#), and the [Medical Toxicology Commons](#)
See next page for additional authors
[Right click to open a feedback form in a new tab to let us know how this document benefits you.](#)

Repository Citation

Chaiprasongsuk, Anyamanee; Janjetovic, Zorica; Kim, Tae-Kang; Jarrett, Stuart G.; D'Orazio, John A.; Holick, Michael F.; Tang, Edith K. Y.; Tuckey, Robert C.; Panich, Uraivan; Li, Wei; and Slominski, Andrzej T., "Protective Effects of Novel Derivatives of Vitamin D₃ and Lumisterol Against UVB-Induced Damage in Human Keratinocytes Involve Activation of Nrf2 and p53 Defense Mechanisms" (2019). *Toxicology and Cancer Biology Faculty Publications*. 88.
https://uknowledge.uky.edu/toxicology_facpub/88

This Article is brought to you for free and open access by the Toxicology and Cancer Biology at UKnowledge. It has been accepted for inclusion in Toxicology and Cancer Biology Faculty Publications by an authorized administrator of UKnowledge. For more information, please contact UKnowledge@lsv.uky.edu.

Protective Effects of Novel Derivatives of Vitamin D₃ and Lumisterol Against UVB-Induced Damage in Human Keratinocytes Involve Activation of Nrf2 and p53 Defense Mechanisms

Digital Object Identifier (DOI)

<https://doi.org/10.1016/j.redox.2019.101206>

Notes/Citation Information

Published in *Redox Biology*, v. 24, 101206, p. 1-19.

This is an open access article under the CC BY-NC-ND license (<http://creativecommons.org/licenses/by-nc-nd/4.0/>).

Authors

Anyamanee Chaiprasongsuk, Zorica Janjetovic, Tae-Kang Kim, Stuart G. Jarrett, John A. D'Orazio, Michael F. Holick, Edith K. Y. Tang, Robert C. Tuckey, Uraivan Panich, Wei Li, and Andrzej T. Slominski



Protective effects of novel derivatives of vitamin D₃ and lumisterol against UVB-induced damage in human keratinocytes involve activation of Nrf2 and p53 defense mechanisms



Anyamanee Chaiprasongsuk^{a,e}, Zorica Janjetovic^a, Tae-Kang Kim^a, Stuart G. Jarrett^b, John A. D'Orazio^b, Michael F. Holick^c, Edith K.Y. Tang^d, Robert C. Tuckey^d, Uraivan Panich^e, Wei Li^f, Andrzej T. Slominski^{a,g,*}

^a Department of Dermatology, University of Alabama at Birmingham, USA

^b Department of Toxicology and Cancer Biology, The Markey Cancer Center, College of Medicine, University of Kentucky, Lexington, KY, USA

^c Department of Medicine, Boston University, MA, USA

^d School of Molecular Sciences, The University of Western Australia, Perth, WA, Australia

^e Department of Pharmacology, Faculty of Medicine Siriraj Hospital, Mahidol University, Bangkok, Thailand

^f Department of Pharmaceutical Sciences, University of Tennessee Health Science Center, Memphis, TN, USA

^g VA Medical Center, Birmingham, AL, USA

ARTICLE INFO

Keywords:

Epidermal keratinocytes
Lumisterol (L₃)
Nuclear factor E2-related factor 2 (Nrf2)
Photoprotective effects
Ultraviolet B (UVB)
Vitamin D₃ hydroxy-derivatives

ABSTRACT

We tested whether novel CYP11A1-derived vitamin D₃- and lumisterol-hydroxyderivatives, including 1,25(OH)₂D₃, 20(OH)D₃, 1,20(OH)₂D₃, 20,23(OH)₂D₃, 1,20,23(OH)₃D₃, lumisterol, 20(OH)L₃, 22(OH)L₃, 20,22(OH)₂L₃, and 24(OH)L₃, can protect against UVB-induced damage in human epidermal keratinocytes. Cells were treated with above compounds for 24 h, then subjected to UVB irradiation at UVB doses of 25, 50, 75, or 200 mJ/cm², and then examined for oxidant formation, proliferation, DNA damage, and the expression of genes at the mRNA and protein levels. Oxidant formation and proliferation were determined by the DCFA-DA and MTS assays, respectively. DNA damage was assessed using the comet assay. Expression of antioxidative genes was evaluated by real-time RT-PCR analysis. Nuclear expression of CPD, phospho-p53, and Nrf2 as well as its target proteins including HO-1, CAT, and MnSOD, were assayed by immunofluorescence and western blotting. Treatment of cells with the above compounds at concentrations of 1 or 100 nM showed a dose-dependent reduction in oxidant formation. At 100 nM they inhibited the proliferation of cultured keratinocytes. When keratinocytes were irradiated with 50–200 mJ/cm² of UVB they also protected against DNA damage, and/or induced DNA repair by enhancing the repair of 6-4PP and attenuating CPD levels and the tail moment of comets. Treatment with test compounds increased expression of Nrf2-target genes involved in the antioxidant response including *GR*, *HO-1*, *CAT*, *SOD1*, and *SOD2*, with increased protein expression for HO-1, CAT, and MnSOD. The treatment also stimulated the phosphorylation of p53 at Ser-15, increased its concentration in the nucleus and enhanced Nrf2 translocation into the nucleus. In conclusion, pretreatment of keratinocytes with 1,25(OH)₂D₃ or CYP11A1-derived vitamin D₃- or lumisterol hydroxy-derivatives, protected them against UVB-induced damage via activation of the Nrf2-dependent antioxidant response and p53-phosphorylation, as well as by the induction of the DNA repair system. Thus, the new vitamin D₃ and lumisterol hydroxy-derivatives represent promising anti-photodamaging agents.

Abbreviations: 1,25(OH)₂D₃, 1α,25-dihydroxyvitamin D₃; 20(OH)D₃, 20S-hydroxyvitamin D₃; 1,20(OH)₂D₃, 1α,20S-dihydroxyvitamin D₃; 20,23(OH)₂D₃, 20S,23S-dihydroxyvitamin D₃; 1,20,23(OH)₃D₃, 1α,20S,23S-trihydroxyvitamin D₃; L₃, lumisterol; 20(OH)L₃, 20-hydroxylumisterol; 22(OH)L₃, 22-hydroxylumisterol; 20,22(OH)₂L₃, 20,22-dihydroxylumisterol; 24(OH)L₃, 24-hydroxylumisterol; Nrf2, transcription factor NF-E2-related factor 2; GSTP1, glutathione S transferase protein 1; GCS, glutamylcysteine synthetase; GPx, glutathione peroxidase; GR, glutathione reductase; HO-1, heme oxygenase-1; TRN, thioredoxin; TXNRD, thioredoxin reductase cytosolic; CAT, catalase; CuZnSOD, superoxide dismutase/Cu/Zn; MnSOD, superoxide dismutase/Mn; MCT4, monocarboxylate transporter 4; CYCB, cyclophilin B; CPD, cyclobutane-pyrimidine dimers; 6-4PP, 6-4 photoproduct; NER, nucleotide excision repair; CYP, cytochrome P450 enzymes; ARE, Antioxidant Response Element; HEKn, human epidermal keratinocytes; EtOH, ethanol; UVB, ultraviolet B

* Corresponding author. Department of Dermatology, University of Alabama at Birmingham, Birmingham, AL 35249, USA.

E-mail address: aslominski@uabmc.edu (A.T. Slominski).

<https://doi.org/10.1016/j.redox.2019.101206>

Received 22 March 2019; Received in revised form 13 April 2019; Accepted 15 April 2019

Available online 20 April 2019

2213-2317/ Published by Elsevier B.V. This is an open access article under the CC BY-NC-ND license (<http://creativecommons.org/licenses/by-nc-nd/4.0/>).

1. Introduction

Ultraviolet B (UVB) radiation is a key agent that induces DNA damage by stimulating a variety of mutagenic and cytotoxic DNA lesions, e.g., cyclobutane-pyrimidine dimers (CPDs) [1–4]. CPDs play a role in photocarcinogenesis in skin cells, including keratinocytes [5,6]. The effects of CPD-associated photodamage possibly further contribute to highly characteristic gene mutations in a central tumor suppressor, p53, which is the first step in the induction of skin disorders and skin cancer [7]. The nucleotide excision repair (NER) system protects against cell death and mutations by removing CPD 6-4 pyrimidine photoproducts (6-4PP), the major photoproducts of UVB irradiation [3]. UVB also induces increased formation of reactive oxygen species (ROS) capable of activating the phosphorylation of p53 and inhibiting DNA repair [8]. Cells can protect themselves against the production of UVB-induced ROS by producing several endogenous and exogenous antioxidants [9–12].

Nuclear factor E2-related factor 2 (Nrf2) is a redox-sensitive transcription factor regulating the cellular antioxidant defense against environmental factors, especially UV radiation [6]. Nrf2 plays a beneficial role in protecting skin cells against UV-induced oxidative damage and cellular dysfunction [13]. The transcriptional regulation of the antioxidant defense system is promoted by the Nrf2-Antioxidant Response Element (ARE) signaling pathway which stimulates the expression of phase II detoxification enzymes including glutathione reductase (GR), heme oxygenase-1 (HO-1), catalase (CAT), manganese superoxide dismutase (MnSOD), and copper zinc superoxide dismutase (CuZnSOD) [14]. In addition, DNA damage induced by UVB irradiation is associated with Nrf2-regulated antioxidants responses in skin cells [15,16]. Thus, synthetic compounds, in particular free radical scavengers or natural products targeting Nrf2, have been proposed to be used in skin photoprotection [1,15,17–20].

During UVB exposure, the B ring of 7-dehydrocholesterol (7-DHC) is photolyzed to previtamin D, which in turn isomerizes into vitamin D₃ [21,22]. With prolonged exposure to UVB lumisterol is formed from previtamin D [21,22]. In general, the active forms of vitamin D₃ are synthesized by the consecutive action of cytochrome P450 enzymes (CYPs) [23]. While CYP2R1 and CYP27A1 catalyze the formation of 25(OH)D₃ (25-hydroxyvitamin D₃) in the liver, CYP27B1 produces the 1 α ,25-dihydroxyvitamin D₃ (1,25(OH)₂D₃) in the kidney [24–26]. CYP11A1 initiates novel pathways of vitamin D₃ activation in various organs or tissue, such as skin, peripheral tissue, adrenals, placenta, gastrointestinal (GI) tract, and several cancer cells of different origin [23,27–33]. Carbons in the side chain of vitamin D₃ at positions 17, 20, 22 and 23 can be hydroxylated by CYP11A1 to produce a variety of metabolites including 20(OH)D₃ and 20,23(OH)₂D₃, which can further

be hydroxylated by CYP27B1 to produce 1,20(OH)₂D₃ and 1,20,23(OH)₃D₃. Interestingly, the active form of vitamin D, 1,25(OH)₂D₃, is reported to protect against oxidative stress [34,35] and to modulate DNA damage/repair systems [36–38], as well as Nrf2 activation [34,39]. Like 1,25(OH)₂D₃, CYP11A1-derived vitamin D₃ derivatives (e.g. 20(OH)D₃) and their down-stream metabolites show anti-proliferative effects against normal and malignant melanocytes and keratinocytes, as well as pro-differentiation and anti-inflammatory effects [40–42]. CYP11A1 also initiates lumisterol (L₃) metabolism through sequential hydroxylation of its side chain [23,43–46]. This leads to the cutaneous production of several hydroxy forms of L₃, including 20(OH)L₃, 22(OH)L₃, 20,22(OH)₂L₃, and 24(OH)L₃ [23,43–45]. Our previous study indicated that treatment with 1,25(OH)₂D₃ or 20(OH)D₃ prior to UVB exposure, protects human keratinocytes from UVB-induced damage by the reduction of CPD levels and stimulation of the expression of p53 phosphorylated at Ser-15 [47]. Importantly, we also found that CYP11A1-derived hydroxylumisterols (20(OH)L₃, 22(OH)L₃, 24(OH)L₃ and 20,22(OH)₂L₃) inhibit the proliferation of epidermal keratinocytes and stimulate their differentiation. In addition, 20(OH)L₃ induced expression of several genes associated with protection against oxidative stress [45].

Since the protective role of the classical active form of vitamin D₃ (1,25(OH)₂D₃) against radiation and UVB-induced damages is recognized [36,38,48,49] and Nrf2 is described as a key regulator of the cellular antioxidant defense against UVB-induced oxidative damage [6,50], we tested the ability of novel CYP11A1-derived vitamin D₃ and lumisterol hydroxy-derivatives to protect primary human keratinocytes against radiation and UVB-induced damage, and the involvement of Nrf2. Therefore, 1,25(OH)₂D₃, CYP11A1-derived metabolites: 20(OH)D₃, 1,20(OH)₂D₃, 20,23(OH)₂D₃, and 1,20,23(OH)₃D₃; lumisterol and its hydroxy-derivatives, including 20(OH)L₃, 22(OH)L₃, 20,22(OH)₂L₃, and 24(OH)L₃, were tested as anti-photodamaging agents targeting Nrf2 (see Graphical abstract).

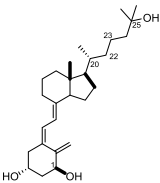
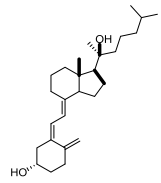
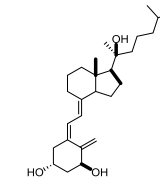
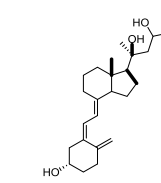
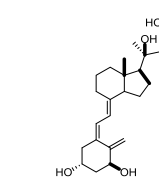
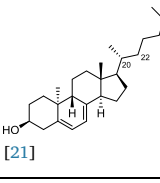
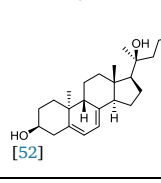
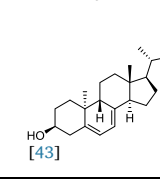
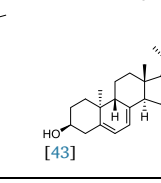
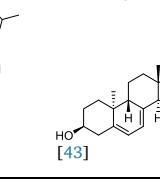
2. Materials and methods

2.1. Source of compounds tested

1,25-dihydroxyvitamin D₃ (1,25(OH)₂D₃) was purchased from Sigma-Aldrich (St. Louis, MO). Lumisterol (L₃) was purchased from Toronto Research Chemicals (North York, ON). Hydroxy-derivatives of vitamin D₃, including 20(OH)D₃, 1,20(OH)₂D₃, 20,23(OH)₂D₃, and 1,20,23(OH)₃D₃, and hydroxy-derivatives of lumisterol, including 22(OH)L₃, 20,22(OH)₂L₃, and 24(OH)L₃, were enzymatically synthesized as described previously [43,45,51]. In addition, 20(OH)D₃ and 20(OH)L₃ were chemically or photochemically synthesized as described

Table 1

Chemical structures of hydroxyderivatives of vitamin D₃ and lumisterol tested in this study. The number indicates the carbon number in the core structures.

Vitamin D ₃ Hydroxyderivatives	1,25(OH) ₂ D ₃	20(OH)D ₃	1,20(OH) ₂ D ₃	20,23(OH) ₂ D ₃	1,20,23(OH) ₃ D ₃
Chemical Structures					
References	[22]	[32,52]	[107,108]	[31,109]	[109,110]
Lumisterol Hydroxyderivatives	lumisterol	20(OH)L ₃	22(OH)L ₃	20,22(OH) ₂ L ₃	24(OH)L ₃
Chemical Structures					
References	[21]	[52]	[43]	[43]	[43]

previously [52,53]. Chemical structures of hydroxyderivatives of vitamin D₃ and lumisterol are in Table 1.

2.2. Cell culture and treatment

Human epidermal keratinocytes (HEKn) were isolated from neonatal foreskin of African-American donors using 2.5 UI/ml dispase and cultured for experiments as previously described [42,54]. Cells were grown in EpiGRO™ human epidermal keratinocyte media supplemented with EpiGRO™ human epidermal keratinocyte complete media kit (Millipore, USA) on collagen-coated plates. Keratinocytes in their third passage were used for the experiments. For the experiments with UVB, media were replaced with phosphate buffered saline (PBS) prior the exposure. Pre-treatment and post-treatment protocols were applied in this study as shown in the graphical abstract. HEKn cells were treated with vitamin D₃ and lumisterol hydroxy-derivatives before UVB irradiation (pre-treatment) for 24 h, or immediately after UVB irradiation (post-treatment). The compounds being tested were diluted in keratinocyte media supplemented with 0.5% BSA solution. A UV transilluminator 2000 from Bio-RAD Laboratories was used for UVB irradiation with UV spectra reported previously [47]. UVB was used at the dose of 25, 50, 75, or 200 mJ/cm². After UVB treatment, cells were incubated in fresh medium supplemented with the same derivatives for additional time, as indicated.

2.3. Measurement of intracellular oxidant formation using the DCFDA assay

HEKn cells were seeded at a density of 3000 cells per well onto 96-well plates in complete media. Once 80% confluence was attained, cells were treated with 1,25(OH)₂D₃, 20(OH)D₃, 1,20(OH)₂D₃, 20,23(OH)₂D₃, 1,20,23(OH)₃D₃, lumisterol, 20(OH)L₃, 22(OH)L₃, 20,22(OH)₂L₃, or 24(OH)L₃ at concentrations of 1 or 100 nM, or with ethanol (vehicle, dilution 1:1000) for 24 h before UVB irradiation (pre-treatment). After incubation, cells were rinsed with cold 1 × PBS. CM-H2DCFDA dye (Molecular Probes, Invitrogen, Eugene, Oregon) diluted in 5 μM HEPES was added and cells were incubated for an additional 30 min at 37 °C. After the pre-incubation with CM-H2DCFDA dye, cells were irradiated with 50 mJ/cm² of UVB and further incubated at 37 °C for 4 h, and subsequently washed with PBS. The generation of ROS was determined by measuring the fluorescence with 480 nm excitation and 528 nm emission, using a Cytation™ 5 cell imaging multi-mode reader (BioTek Instruments, Inc., VT, USA). Data are presented as the percentage of control (EtOH- treated cells).

2.4. Determination of cell proliferation using the MTS assay

HEKn cells were plated onto 96-well plates. The following day, cells were treated individually with all the compounds being tested (see above) at concentrations of 1, 10, or 100 nM, or with the ethanol vehicle (dilution 1:1000), for 24 h before UVB irradiation (pre-treatment) or immediately after UVB irradiation (post-treatment). HEKn cells plated and treated as described above were then irradiated with 25 mJ/cm² of UVB and further incubated in fresh medium supplemented with the same vitamin D₃ or lumisterol hydroxy-derivatives for an additional 24 h. After incubation, MTS Reagents was added (20 μl/well) and cells incubated for 3 h at 37 °C under standard culture conditions. The absorbance was recorded at 490 nm using a Cytation™ 5 cell imaging multi-mode reader (BioTek Instruments, Inc., VT, USA). Data are presented as the relative absorbance at 490 nm compared with control (EtOH-treated) cells.

2.5. Measurement of DNA damage using the comet assay

The comet assay was performed following the manufacturer's protocol (Trevigen, Gaithersburg, MD). HEKn cells were plated in 12-well

plates and treated individually with all of the above mentioned compounds at a concentration of 100 nM, or ethanol vehicle (dilution 1:1000), for 24 h before UVB irradiation (pre-treatment). The medium was then replaced with 1 × PBS and cells were exposed to UVB, 200 mJ/cm². PBS was removed and replaced with fresh medium supplemented with the same vitamin D₃ or lumisterol hydroxy-derivatives for an additional 3 h at 37 °C. After detaching, cells were counted and used for the comet assay. Cell suspensions at a density of 1 × 10⁵/ml were then mixed with molten 1.2% low-melting-point agarose (dilution 1:10) at 37 °C and a 15 μL aliquot was placed onto two frosted slides pre-coated with 0.6% normal agarose, and incubated at 4 °C for 30 min. After the gel had solidified the cells were digested in cooled lysis solution at 4 °C for 1 h. DNA strand breaks were separated by electrophoresis in alkaline solution (200 mM NaOH, 1 mM EDTA, pH > 13) in a horizontal gel electrophoresis slide tray (Comet-10, Thistle Scientific, Glasgow, UK). The DNA with breaks was exposed to alkaline unwinding for 1 h at 4 °C after which electrophoresis was performed at 25 V for 1 h. After electrophoresis, the slides were gently removed from the tray and washed with neutralizing buffer (0.4 M Tris-HCl, pH 7.5) for 5 min. The slides were immersed twice in distilled H₂O for 5 min each and then dehydrated in 70% ethanol for 5 min. Finally, the comets on the slides were stained and visualized with 20 μg/ml propidium iodide (Sigma-Aldrich, St. Louis, MO). The slides were examined and images were captured using a Cytation™ 5 cell imaging multi-mode reader. Approximately 60 comet images were taken for each condition. DNA damage was measured by the tail length using Comet Score software available from <http://www.scorecomets.com>. Data are presented as mean tail moment compared with the control (EtOH- treated cells).

2.6. Analysis of DNA repair

HEKn cells were cultured for three days in 60 mm petri dishes (TPP® tissue culture dishes, MidSci, St. Louis, MO). Cells were treated individually with vitamin D₃ or lumisterol hydroxy-derivatives at a concentration of 100 nM, or with ethanol vehicle (dilution 1:1000), for 24 h before UVB irradiation (pre-treatment). After the treatment, cells were irradiated with either 25 mJ/cm² or 50 mJ/cm² of UVB and further incubated in fresh media with the same hydroxy-derivative for an additional 1 or 3 h. For the preparation of cell lysates, cells were detached using trypsin reagents and centrifuged at 11,200 × g for 10 min at 4 °C. Cell pellets were then collected and stored at −80 °C. DNA was isolated (DNeasy, Qiagen), heat-denatured at 100 °C for 10 min, applied to a Hybond nitrocellulose membrane (Amersham) using a vacuum-driven slot blot apparatus, and fixed by baking for 1 h at 80 °C. Membranes were incubated with mouse monoclonal antibodies specific for 6–4 photoproducts (1/10,000) and CPDs (1/10,000) (Cosmo Bio Co. Cat# NMDND002). Peroxidase-conjugated anti-mouse secondary antibody was used at a dilution of 1/10,000 in blocking buffer. For acquisition analysis, a Storm 860 was used and membranes scanned using channel 2 with blue excitation at 450 nm and emission at 520 nm, sensitivity was set to normal and PMT voltage set to 400 V. Percent repair was determined as the extent of repair between 1 h post-UVB exposure and 3 h post-UVB exposure [55,56].

2.7. Immunofluorescence analysis of nuclear/cytosolic Nrf2 ratio and its target proteins (CAT, HO-1 and MnSOD) expression as well as expression of CPD and phosphorylated p53

HEKn cells were plated onto 96-well plates and at 80% confluence were treated with the vitamin D₃ or lumisterol hydroxy-derivatives at a concentration of 100 nM, or ethanol vehicle (dilution 1:1000), for 24 h before UVB irradiation (pre-treatment). Cells were then irradiated with 50 mJ/cm² of UVB and further incubated in fresh medium supplemented with the same derivative for an additional time as indicated (post-treatment). Nrf2 nuclear translocation was measured 24 h post-UVB irradiation, while Nrf2 target proteins (CAT and HO-1) and

MnSOD were measured 3 h post-UVB irradiation and 1 h post-UVB irradiation, respectively. For the DNA damage pathway, CPD and phosphor-p53 (Ser15) were measured at 3 h post-UVB irradiation and 1 h post-UVB irradiation, respectively. Cells were fixed in 4% paraformaldehyde (PFA) for 10 min at room temperature and washed three times with 0.1% Triton X-100 (BioRad, Hercules, CA, USA) in PBS. Blocking solution (1% BSA in PBS) was added into each well and cells incubated for 1 h at room temperature. Cells were then incubated with primary antibody (dilution 1:100) in blocking solution overnight at 4 °C. The following day cells were washed and incubated for 1 h at RT with a specific secondary antibody, Alexa-Fluor 488, (Invitrogen Molecular Probes, Eugene, Oregon, USA) diluted 1:100 in blocking solution. After washing with PBS, nuclei were stained red with propidium iodide (Vector Laboratories, Burlingame, CA). Stained cells were imaged at 40X magnification and analysed with Gen 5.0 software with a Cytation™ 5 cell imaging multi-mode reader. Fluorescence intensity of the images was analysed using ImageJ software. Alexa-Fluor 488 dye-labeled proteins were separately detected through a green fluorescence channel. Quantitative data from ImageJ and pixel intensities of the image were then imported into Microsoft Excel for generating the percentage (mean \pm SD) of control (ethanol without UVB or ethanol with UVB).

To determine the nuclear to cytosolic ratio, the fluorescent intensity of the cell nuclei was measured separately from the fluorescence of the whole cells. Fluorescent staining in cytosolic fractions was calculated by subtracting nuclear staining from whole cell staining. The ratio of nuclear and cytosolic fractions was calculated as previously described [57,58] and shown in histograms as the mean of the fold change \pm SD.

2.8. Quantitative real-time reverse transcriptase-polymerase chain reaction (qRT-PCR) for measurement of mRNA expression

HEKn cells were cultured for three days in 60 mm petri dishes and treated individually with the vitamin D₃ or lumisterol hydroxy-derivatives at a concentration of 100 nM, or ethanol vehicle (dilution 1:1000) for 24 h before UVB irradiation (pre-treatment). Cells were then irradiated with 50 mJ/cm² of UVB and further incubated in fresh medium supplemented with the same derivative for an additional 24 h. For preparation of cell lysate, cells were detached using trypsin and centrifuged at 11,200 \times g for 10 min at 4 °C. Cell pellets were then collected and total RNA was isolated using the absolutely RNA RT-PCR Miniprep kit (Stratagene, La Jolla, CA). Reverse transcription was carried out with 1 μ g of total RNA using the Improm-II reverse transcriptase (Promega, Madison, WI, USA) under the conditions described in the manual. The reverse transcription reaction was performed using a High Capacity cDNA reverse transcription Kit (Applied Biosystems, Foster City, CA). PCR reactions were performed in triplicate using a LightCycler 480 Probes Master (Roche Applied Science, Indianapolis, IN) under the following amplification conditions: 95 °C for 15 s, 60 °C for 30 s, and 72 °C 10 s for 35 cycles. Real-time RTPCR was performed in a total volume of 10 μ l containing 2 μ l cDNA template with Kapa SYBR Fast qPCR Master Mix (Kapa Biosystems, Boston, MA) and 1 μ M primer mix. Sequences of PCR primer sets for the genes studied are shown in [Supplemental Table 1](#). The mRNA levels were normalized with reference to the amount of housekeeping gene transcripts (β -actin, cyclophilin, or GAPDH mRNA) using the $\Delta\Delta$ Ct method. Changes in gene expressions are presented as the mean of fold-change with statistically significant differences indicated. The Student t-test was used for the comparison with non-irradiated or irradiated control cells, The P value is reported as * P < 0.05, **P < 0.01, ***P < 0.001. A heat map was generated using Prism (GraphPad Software Inc.).

2.9. Western blot analysis of Nrf2 and phosphorylated p53 expression

Western blotting was carried out using nuclear extracts for detection of Nrf2 nuclear localization and phosphorylated p53. HEKn cells were

cultured in 100 mm petri dishes and treated individually with the vitamin D₃ and lumisterol hydroxy-derivatives at a concentration of 100 nM, or with ethanol vehicle (dilution 1:1000), for 24 h before UVB irradiation (pre-treatment). After exposure to 50 mJ/cm² of UVB, cells were further incubated in fresh medium supplemented with the same hydroxy-derivative for an additional 24 h. Cells were washed with ice-cold PBS mixed with phosphatase inhibitors and removed from the dish by scraping. Cell pellets were transferred into micro-centrifuge tubes and centrifuged at 2000 \times g for 5 min. Cell pellets were then suspended in 200 μ l of 1X hypotonic buffer (Active motif, Carlsbad, CA, USA) and incubated on ice for 15 min. Lysate mixtures were centrifuged at 14,000 \times g for 30 s at 4 °C and the supernatant collected as the cytosolic fraction. Nuclear pellets were then resuspended in 50 μ l of complete lysis buffer containing 2.5 μ l of detergent for solubilizing membranes. The mixtures were incubated on ice with intermittent vortexing for 30 min, centrifuged at 14,000 \times g for 10 min and the supernatant collected as the nuclear fraction. The protein concentration of cytosolic and nuclear fractions was measured using the Bradford method (BioRad, Hercules, CA, USA).

Proteins were separated using a Mini-PROTEAN® TGX™ gel (BioRad, Hercules, CA, USA) and transferred onto a PVDF membrane. Membranes were blocked with 5% skim milk (Tris-buffer saline containing 0.1% (v/v) Tween 20 and 5% (w/v) skim milk) for 1 h and then incubated overnight at 4 °C with the rabbit polyclonal antibody against Nrf2 (sc-722, Santa Cruz Biotechnology; 1:500 dilution) or rabbit polyclonal phosphor-p53 (Ser-15) (9284S, Cell signaling; 1:2000 dilution) in 5% skim milk. After three washes with TBST (Tris-buffer saline containing 0.1% (v/v) Tween 20) for 10 min each, membranes were incubated for 1 h at room temperature with the HRP-conjugated secondary antibodies (ab6721 for anti-rabbit IgG and ab6741 for anti-goat IgG HRP labeled secondary antibody, Abcam; 1:3000 dilution) in TBST. Immuno-reactivity was detected using the Bio-Rad ECL kit Supersignal West Pico Chemiluminescent Substrate (Pierce). Protein expression was normalized relative to that of loading controls; B-actin-peroxidase (A3854, Sigma; 1:5000 dilution) for the cytosolic fraction and Lamin A/C (N-18) (sc6215, Santa Cruz Biotechnology, 1:2000 dilution) for the nuclear fraction. The integrated optical density of the bands was analysed by ImageJ software (NIH free download).

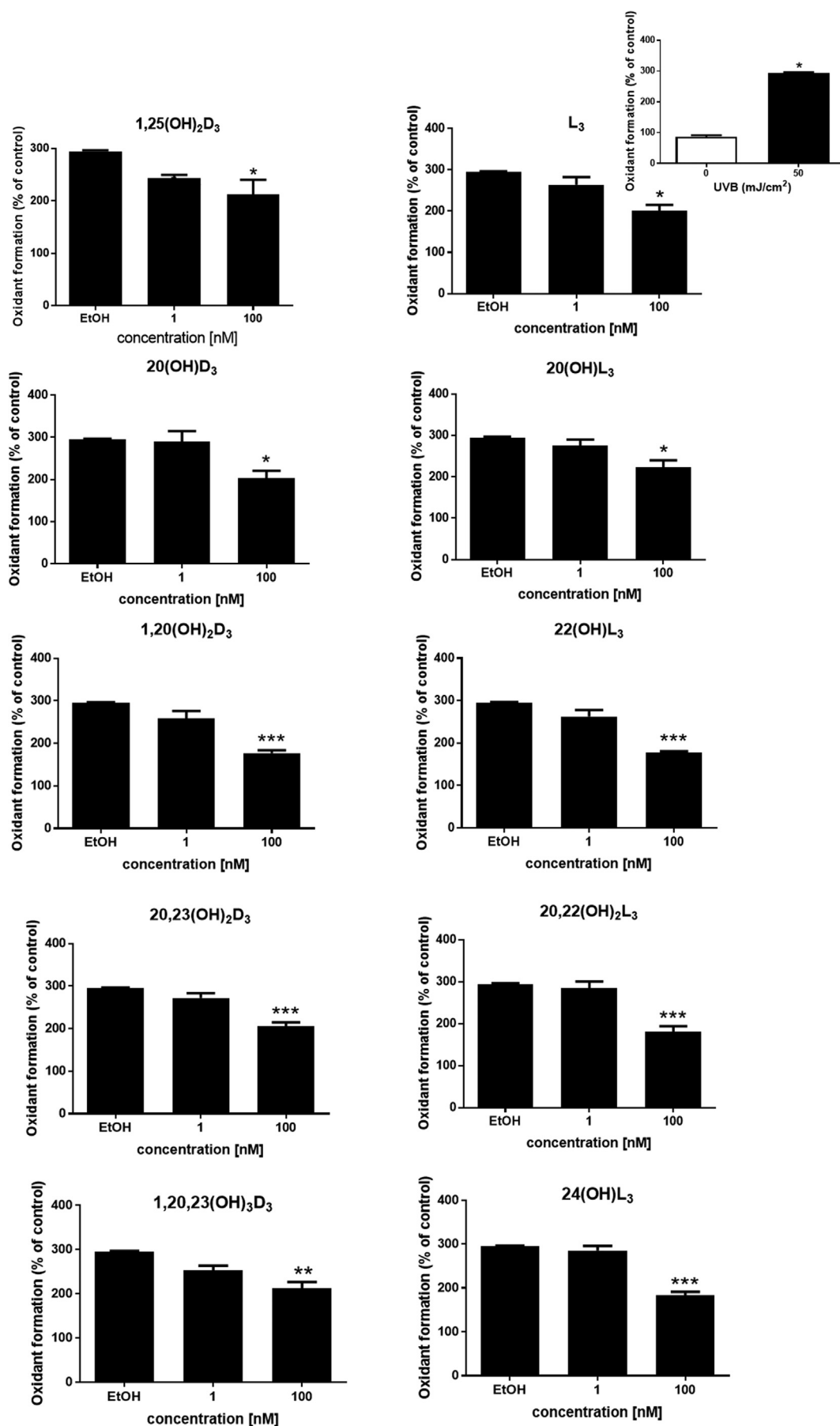
3. Statistical analysis

Data are expressed as mean \pm standard deviation of at least three separate experiments ($n \geq 3$) performed on different days using freshly prepared reagents. The significance of non-irradiated controls or individual treatment groups in comparison to the UVB-irradiated groups was evaluated by the student t-test. The significance of non-irradiated controls in comparison to each compound tested at various doses was evaluated by one-way analysis (ANOVA) using Prism (GraphPad Software Inc.).

4. Results

4.1. Novel hydroxy-derivatives of vitamin D₃ and lumisterol reduce oxidant formation by UVB-irradiated keratinocytes

It has previously been established that 1,25(OH)₂D₃ and 20(OH)L₃ protect against ROS formation [34,35,45]. In this study we tested vitamin D₃ and lumisterol metabolites: 20(OH)D₃, 1,20(OH)₂D₃, 20,23(OH)₂D₃, 1,20,23(OH)₃D₃, lumisterol, 20(OH)L₃, 22(OH)L₃, 20,22(OH)₂L₃, and 24(OH)L₃, as protective agents against UVB-induced oxidative stress in cells, in comparison to 1,25(OH)₂D₃. HEKn cells were treated individually with each of these derivatives for 24 h prior to UVB irradiation (50 mJ/cm²). For non-irradiated cells treated with the same compounds, only 20(OH)L₃ and 24(OH)L₃ decreased oxidant formation (P < 0.05 and P < 0.01, [Supplemental Fig. 1](#)). At 4 h following irradiation at a UVB dose of 50 mJ/cm², there was substantial induction of



(caption on next page)

Figure 1. Novel derivatives of vitamin D₃ and lumisterol reduce oxidant formation in UVB-irradiated keratinocytes. Keratinocytes were pretreated with the indicated vitamin D₃ and lumisterol hydroxy-derivatives for 24 h prior to UV irradiation (50 mJ/cm²). The irradiated cells were further incubated for an additional 4 h with the hydroxy-derivatives or ethanol vehicle, while non-irradiated cells were treated with the ethanol vehicle (comparison presented as insert, top right). Oxidant formation was examined using the DCFDA reagent at 4 h post UVB irradiation. Data are presented as the percentage of the control (mean ± SD). The statistical significance of differences was evaluated by one-way ANOVA, * P < 0.05, ** P < 0.01, *** P < 0.001 for all conditions.

oxidant formation by irradiated cells as compared to non-irradiated cells (P < 0.05, Fig. 1, top right). Each of the above compounds reversed the UVB-mediated ROS production in a dose-dependent manner (Fig. 1) and at 100 nM, all derivatives significantly reduced oxidant formation by UVB-irradiated cells (P < 0.05, P < 0.01, and P < 0.001, Fig. 1).

4.2. Anti-proliferative effects of novel derivatives of vitamin D₃ and lumisterol

Previously, some studies reported that 1,25(OH)₂D₃, 20(OH)D₃, 20(OH)L₃, 22(OH)L₃, 24(OH)L₃ and 20,22(OH)₂L₃ inhibited proliferation of a variety of cell types, including normal and immortalized human keratinocytes [45,59,60]. In this study, we examined the inhibitory effects of vitamin D₃ and lumisterol derivatives on proliferation of keratinocytes exposed to the UVB (25 mJ/cm²); this did not significantly affect the survival of keratinocytes. Additionally, no significant difference was observed in the cell morphology between ethanol-treated control cells and cells treated with the hydroxy-derivatives (Supplemental Fig. 2). In non-irradiated cells treated with 20(OH)D₃, 1,20(OH)₂D₃, 20,23(OH)₂D₃, 1,20,23(OH)₃D₃, L₃, or 24(OH)L₃ there was a significant inhibition of cell proliferation (P < 0.05 and P < 0.01, Supplemental Fig. 3). A small augmentation of the proliferative effect was found in keratinocytes irradiated with a UVB dose of 25 mJ/cm² in comparison to non-irradiated control cells (P < 0.05, Fig. 2), top right. Moreover, pre-treatment with a range of concentrations of the vitamin D₃ and lumisterol hydroxy-derivatives, as well as lumisterol itself, markedly suppressed the proliferation of keratinocytes exposed to UVB (P < 0.01 and P < 0.001, Fig. 2).

4.3. Novel hydroxy-derivatives of vitamin D₃ and lumisterol can reverse the DNA damage caused by UVB irradiation

Since several reports have documented that UVB irradiation plays a crucial role in DNA damage [3–6], we examined whether treatment with vitamin D₃ or lumisterol derivatives can inhibit UVB-induced DNA damage. We utilized Comet analysis, a well-recognized DNA damage biomarker, to evaluate the protective effects of the compounds under study [61]. UVB irradiation at the dose of 200 mJ/cm² substantially induced DNA damage in irradiated cells as compared to non-irradiated cells (P < 0.001, Fig. 3A, inserted images and graphs). The protective effects of vitamin D₃ or lumisterol derivatives, including lumisterol itself, on UVB-induced DNA damage to cells, was evaluated after incubation with the hydroxy-derivatives for 3 h. As shown in Fig. 3, all the vitamin D₃ and lumisterol derivatives tested exhibited significant and robust restoration of the Comet tail moment in comparison to untreated cells (P < 0.001, Fig. 3B, inserted images and graphs). Additionally, the same treatment of non-irradiated cells had no effect on DNA breakage, as shown in Comet assays in Supplemental Fig. 4.

4.4. The effects of novel derivatives of vitamin D₃ and lumisterol on the repair of 6-4PP

6-4PP is a crucial product of UVB-induced damage to human keratinocytes that is removed through the nucleotide excision repair pathway [3,62–64]. The repair activity resulting in 6-4PP removal was measured to evaluate the photoprotective effects of all compounds under study on UVB-irradiated keratinocytes. Vitamin D₃ derivatives, as well as lumisterol and its derivatives except 24(OH)L₃, enhanced the

percentage of repair of 6-4PP in cells treated with UVB at a dose 25 mJ/cm² compared with UVB (25 mJ/cm²)-irradiated control cells. Similarly, 1,25(OH)₂D₃, 20(OH)D₃, 1,20(OH)₂D₃, 1,20,23(OH)₃D₃, 20(OH)L₃, 22(OH)L₃, 20,22(OH)₂L₃, and 24(OH)L₃ caused the induction of 6-4PP repair in cells treated with UVB at dose 50 mJ/cm² compared with UVB (50 mJ/cm²)-irradiated control cells (Fig. 4). These results indicate that all the compounds under study promote the repair of DNA damage in UVB-irradiated cells, at least at one of the doses of UVB employed.

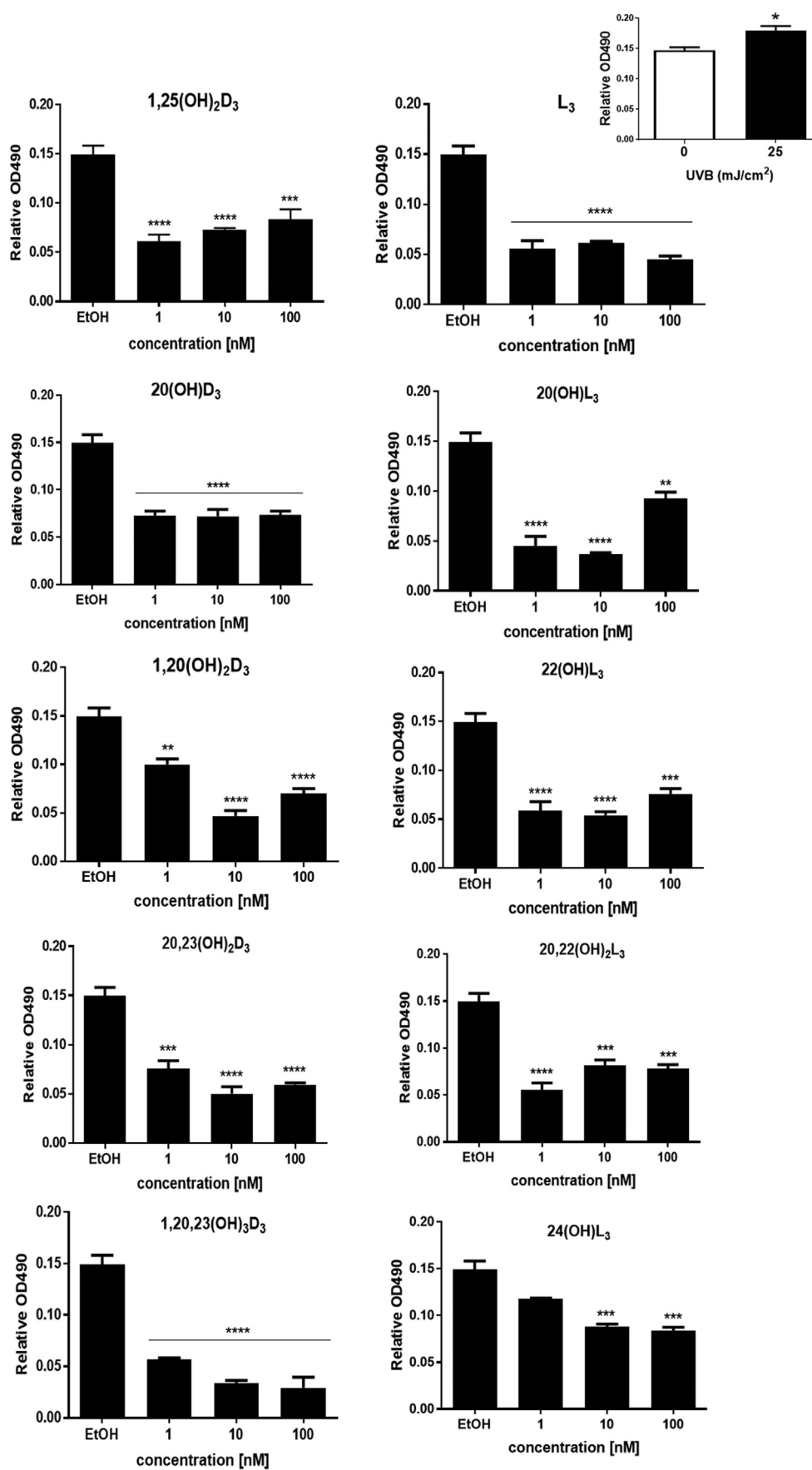
4.5. Treatment with novel derivatives of vitamin D₃ and lumisterol reduced CPD accumulation and stimulated nuclear accumulation of phosphorylated p53

The formation of CPD is considered as one of the markers of DNA damage [3,4]. The DNA repair capacity of cells treated with vitamin D₃ and lumisterol hydroxy-derivatives was measured from their ability to reduce the level of CPD in keratinocytes exposed to UVB. Our previous results revealed a reduction in CPD damage, and stimulation of p53 phosphorylated at Ser-15 in human keratinocytes treated with 1,25(OH)₂D₃ or 20(OH)D₃ prior to UVB exposure [47]. We investigated the protective effects on cells treated with the compounds under study and irradiated with a UVB dose of 50 mJ/cm². At 3 h following UVB irradiation, production of CPD was significantly increased (P < 0.001) (Fig. 5A, left). The treatment with the vitamin D₃ and lumisterol hydroxy-derivatives led to a significant inhibition of CPD production for 1,25(OH)₂D₃, 20(OH)D₃, 1,20(OH)₂D₃, 20,23(OH)₂D₃, 22(OH)L₃, 20,22(OH)₂L₃, and 24(OH)L₃, as shown in a Fig. 5A (right) (P < 0.05).

An underlying factor that may contribute to the effects of CPD on the induction of apoptosis is the status of tumor suppressor p53 in the cell. p53 is a transcription factor playing an important role in cell-cycle control, apoptosis and the response to DNA damage, as well as playing a critical role in protection against carcinogenesis [5]. Therefore, to further investigate the protective effects of vitamin D₃ and lumisterol derivatives against UVB-induced damage, the expression of active p53 (p53 phosphorylated at Ser-15) was assessed. UVB exposure resulted in the accumulation of phosphorylated p53 in the nucleus (P < 0.05) (Fig. 5B, left). Moreover, pre-treatment of keratinocytes with 20(OH)D₃, 1,20(OH)₂D₃, 20,23(OH)₂D₃, L₃, 20(OH)L₃, and 22(OH)L₃, significantly enhanced UVB-stimulated phosphorylated p53(Ser-15) in cell nuclei as shown in Fig. 5B (right) (P < 0.05 and P < 0.01). These results suggest that the photoprotective effects of vitamin D₃ and lumisterol hydroxy-derivatives against skin damage include p53 activation.

4.6. Heat map summary of the gene expression profile for antioxidant signaling in keratinocytes treated with vitamin D₃ or lumisterol hydroxy-derivatives

Our previous study showed that there was a significant induction of the expression of anti-oxidant genes by 20(OH)L₃ in human keratinocytes [45]. To gain a better understanding of the molecular mechanisms of Nrf2-regulated antioxidant gene expression, comparative gene profiling was performed. Several reports indicate that Nrf2 is responsible for the induction of the expression of a vast array of cytoprotective genes, including glutathione S-transferase P1 (GSTP1), gamma-glutamylcysteine synthetase (GCS), glutathione peroxidase (GPx), glucocorticoid receptor (GR), heme oxygenase-1 (HMOX-1), thioredoxin (TRX), thioredoxin reductase (TRXR), catalase (CAT), copper zinc superoxide dismutase (SOD1), manganese superoxide dismutase (SOD2),



(caption on next page)

Fig. 2. Anti-proliferative effect of vitamin D₃ and lumisterol hydroxy-derivatives on UVB-irradiated keratinocytes. UVB-irradiated (25 mJ/cm²) and non-irradiated keratinocytes (comparison presented as insert, top right) were treated with the indicated hydroxy-derivatives for 24 h prior to UV irradiation then incubated with the same hydroxy-derivative for an additional 24 h. A MTS assay was then performed and data analysed by Cytation 5. Data are presented as relative OD490 (mean \pm SD). The statistical significance of differences was evaluated by one-way ANOVA, *P < 0.05, **P < 0.01, ***P < 0.001, ****P < 0.0001 for all conditions.

and monocarboxylate transporter 4 (*MCT4*) [14,50,65,66]. We thus looked at the expression profile of these genes in keratinocytes treated with the vitamin D₃ or lumisterol derivatives and exposed to UVB (50 mJ/cm²).

Gene expression was assessed in keratinocytes 24 h post-UVB irradiation. Ten of the twelve genes examined showed a significant down-regulation (**P < 0.01 and ***P < 0.001) in UVB-irradiated cells compared with non-irradiated control cells. However, *CAT* and *SOD1* were up-regulated (**P < 0.01) in comparison to non-irradiated control cells (Fig. 6A).

Results also revealed that genes downstream of Nrf2 containing an antioxidant response element, including *HMOX-1*, *GPx*, *CAT*, *SOD1*, and

SOD2, generally displayed enhanced expression in non-irradiated cells treated with vitamin D₃ or lumisterol derivatives in comparison to untreated control cells (*P < 0.05, **P < 0.01 and ***P < 0.001) (Fig. 6B, upper map). While a drastic decline in Nrf2-regulated antioxidant genes in response to UVB exposure was generally observed, treatment of keratinocytes with vitamin D₃ or lumisterol derivatives prior to UVB challenge caused strong induction of the expression of *Nrf2* and *GR*, and to a lesser degree *HMOX-1*, and *TRXR* in irradiated cells (*P < 0.05, **P < 0.01 and ***P < 0.001) (Fig. 6B, below part). Additionally, *CAT* and *SOD2* (Superoxide dismutase/Mn; MnSOD) generally showed lower expression with some of the hydroxy-derivatives. 1,20,23(OH)₃D₃ was particularly effective at increasing the

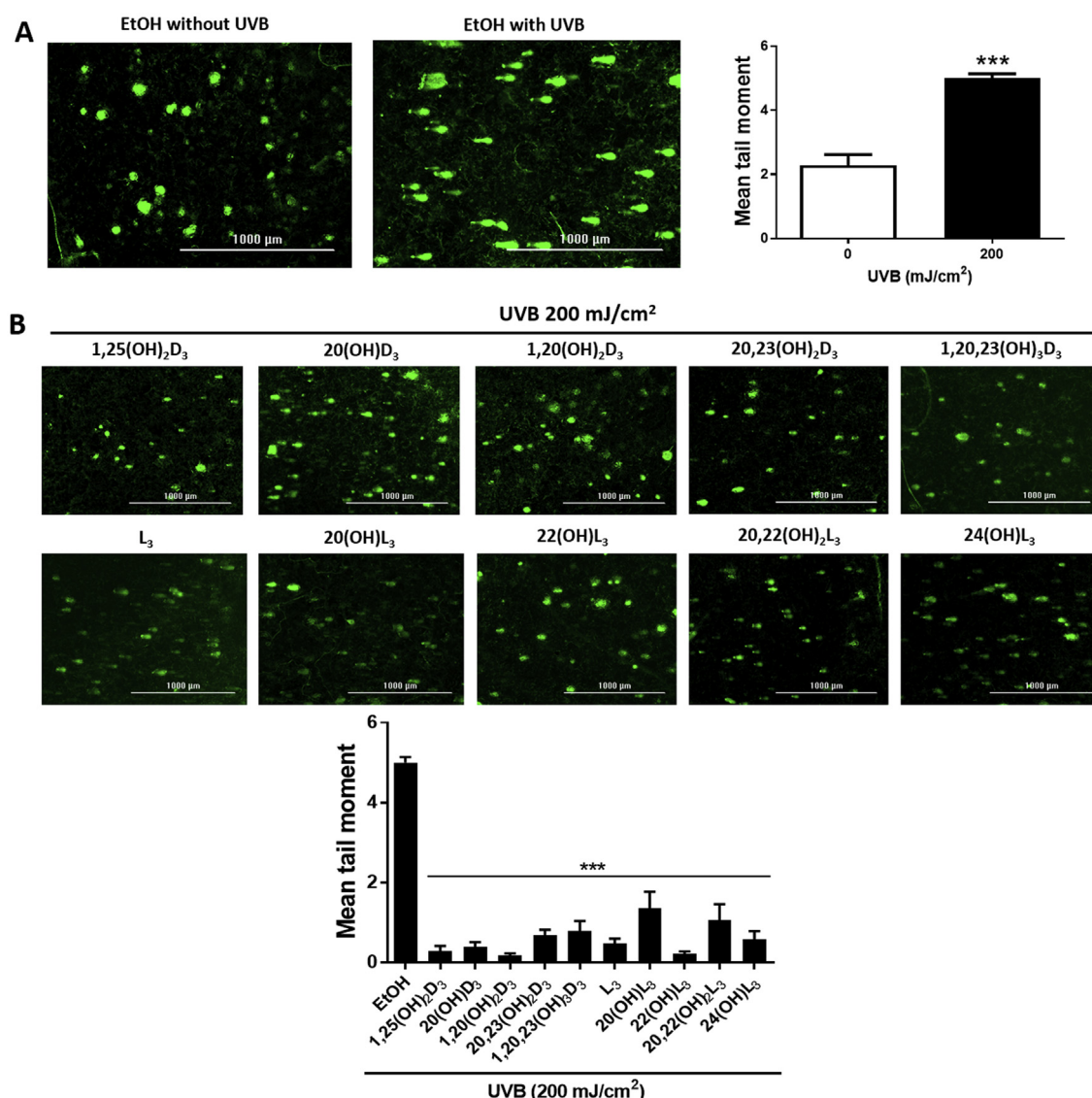


Fig. 3. Novel derivatives of vitamin D₃ and lumisterol reduce DNA damage caused by UVB irradiation. Keratinocytes were pretreated with the indicated hydroxy-derivative of vitamin D₃ or lumisterol (100 nM) for 24 h prior to UV irradiation (200 mJ/cm²), then further incubated with the same hydroxy-derivative for 3 h and subjected to the comet assay. (A), Non-irradiated compared with UVB-irradiated cells without the hydroxy-derivatives; (B) irradiated cells treated with the hydroxy-derivatives. DNA damage was measured as mean tail moment, using Comet score software analysis. Data are presented as the mean tail moment (mean \pm SD). The statistical significance of differences was evaluated by the student t-test, *** P < 0.001 for all conditions.

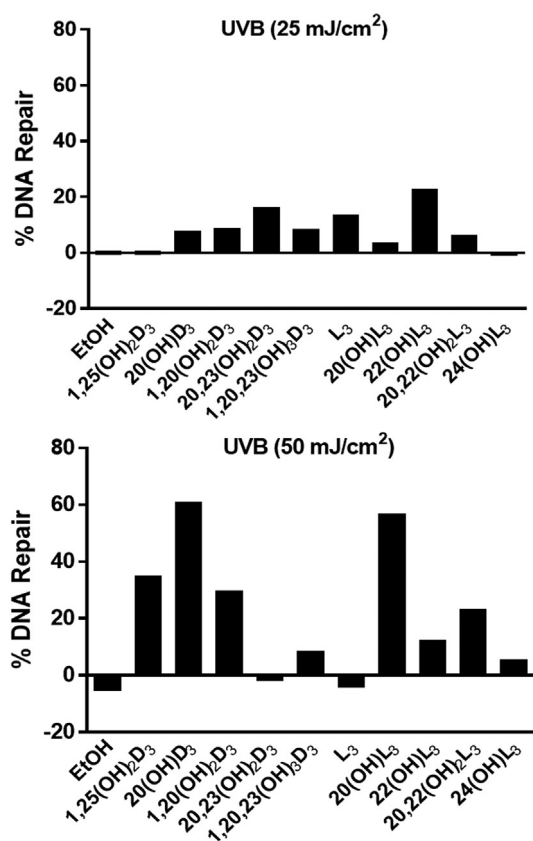


Fig. 4. Novel derivatives of vitamin D₃ and lumisterol enhance the repair of 6-4 photoproducts (6-4PP). HEK cells cultured for three days were pretreated with the indicated hydroxy-derivatives of vitamin D₃ or lumisterol (100 nM), or ethanol vehicle, for 24 h before UVB irradiation at either (A) 25 mJ/cm² or (B) 50 mJ/cm². After irradiation, cells were further incubated in fresh media with the same hydroxy-derivative for an additional 1 or 3 h. The disappearance of 6-4 Photoproducts between 1 and 3 h was used to determine the percent repair.

expression of *GSTP1*, *GCS*, *HMOX-1*, *TRX* and *TRXR* in UV-irradiated cells.

4.7. Novel vitamin D₃ and lumisterol derivatives restore Nrf2-regulated antioxidant defense system in UVB-induced damaged keratinocytes

Our previous studies revealed a significant protective ability of Nrf2 through balancing the oxidative stress status in cells with expression of Nrf2 knocked down [6,15]. Nrf2, a key regulator of the cellular antioxidant defense system, plays a beneficial role in protecting skin cells against UVB-induced DNA damage [13,14,17]. We further examined whether the protection against DNA damage by vitamin D₃ and lumisterol hydroxy-derivatives, involved modulation of Nrf2 nuclear accumulation, as assessed by immunofluorescent labeling of keratinocytes. The intracellular distribution of Nrf2 was assessed by image analysis of stained cells. At 24 h post-irradiation, UVB (50 mJ/cm²) was found to mediate a decrease in Nrf2 nuclear accumulation (Fig. 7A, images and graph). 20(OH)D₃, 1,20(OH)₂D₃ and 1,20,23(OH)₃D₃, lumisterol, 20(OH)L₃, 22(OH)L₃ and 20,22(OH)₂L₃ increased the nuclear/cytosolic Nrf2 ratio compared to UV-irradiated control cells. (Fig. 7B, images and middle graph). Treatment with all the hydroxy-derivatives under study also led to an increase of nuclear/cytosolic Nrf2 ratio in non-irradiated cells (Supplemental Fig. 5).

Since, Nrf2-antioxidant signaling has a well-established key role in protection against UV-mediated skin damage [17,56], we further investigated the protective effect of the vitamin D₃ and lumisterol derivatives against UVB-mediated oxidative stress by Nrf2-regulated

antioxidant responses. A marked reduction in catalase ($P < 0.001$, Fig. 8A, top right) and HO-1 ($P < 0.001$, Fig. 8B, top right) protein levels in UVB-irradiated cells was observed at 3 h post-irradiation, while MnSOD ($P < 0.001$, Fig. 8C, top right) protein expression was drastically decreased at 1 h post-irradiation, as compared to non-irradiated cells. While a decline in catalase and HO-1 protein expression in response to UVB exposure was observed, treatment with all the vitamin D₃ and lumisterol hydroxy-derivatives except 20(OH)L₃ and 24(OH)L₃ in the case of catalase, and 20(OH)L₃ and 20,22(OH)₂L₃ in the case of HO-1, prior to the UVB challenge, led to a significant induction of expression compared to ethanol-treated control cells ($P < 0.01$ and $P < 0.001$, Fig. 8A; $P < 0.05$, $P < 0.01$, and $P < 0.001$, Fig. 8B). Additionally, cells pre-treated with 20,23(OH)₂D₃, or lumisterol, displayed elevated levels of MnSOD compared to ethanol-treated control cells, despite the initial reduction caused by UVB irradiation in untreated control cells ($P < 0.01$, Fig. 8C). Furthermore, all derivatives except 22(OH)L₃ elevated catalase protein levels (Supplemental Fig. 6A). Also, 1,25(OH)₂D₃, 20(OH)D₃, 1,20(OH)₂D₃, 20,22(OH)₂L₃, and 24(OH)L₃ induced HO-1 protein expression (Supplemental Fig. 6B), while 1,25(OH)₂D₃, 20,23(OH)₂D₃, and 1,20,23(OH)₃D₃ also increase MnSOD protein levels in non-irradiated cells (Supplemental Fig. 6C).

4.8. Quantitative Western blot analyses of nuclear and cytoplasmic location of Nrf2 and phosphorylated p53 proteins following treatment with vitamin D₃ or lumisterol hydroxy-derivatives

To confirm the effects on the intracellular distribution of Nrf2 (Fig. 7) and phosphorylated p53 (Fig. 5B) determined by immunofluorescent staining, we performed quantitative blotting analyses. Keratinocytes were pre-treated for 24 h with vitamin D₃ and lumisterol derivatives and then exposed to UVB (50 mJ/cm²). The intensity of Nrf2 protein bands (68 kDa, indicated by a black arrow) was quantified using ImageJ. An increase in the ratio of nuclear versus cytosolic Nrf2 protein indicates that there has been an increase in nuclear translocation of Nrf2. The nuclear/cytosolic Nrf2 ratio decreased by approximately 40% in UVB-irradiated cells when compared to non-irradiated cells ($P < 0.01$, Fig. 9A, top right). Treatment with all the compounds under study except 1,25(OH)₂D₃, 22(OH)L₃ and 20,22(OH)₂L₃ significantly increased the nuclear/cytosolic Nrf2 ratio in cells exposed to UVB in comparison to irradiated-control cells ($P < 0.05$ and $P < 0.01$, Fig. 9A).

The nuclear accumulation of p53 promotes cell cycle arrest to allow DNA repair process. The intensity of Phosphorylated-p53 (Ser-15) protein bands (53 kDa, indicated by a black arrow) was quantified using ImageJ. UVB irradiation, at dose 50 mJ/cm², directly stimulated phosphorylated p53 protein levels in the nuclear fraction ($P < 0.01$, Fig. 9B, top right). Treatment with 1,25(OH)₂D₃, 1,20(OH)₂D₃, 1,20,23(OH)₃D₃, lumisterol, 20(OH)L₃, 22(OH)L₃, and 20,22(OH)₂L₃ enhanced nuclear p53 level in cells exposed to UVB ($P < 0.05$, Fig. 9B).

4.9. Effects of post-treatment with novel derivatives of vitamin D₃ or lumisterol on Nrf2-regulated antioxidant responses in human keratinocytes exposed to UVB irradiation

In addition to characterizing the protective effects of the vitamin D-related derivatives administered prior to UVB irradiation, we also examined whether they had beneficial post-treatment effects [67]. Keratinocytes were exposed to a UVB dose of 50 mJ/cm² and then immediately treated with the same set of vitamin D₃ and lumisterol hydroxy-derivatives described above, at a concentration of 100 nM for 24 h. There was a significant increase in Nrf2 protein expression in the nucleus relative to the cytoplasm following the treatment of UV-irradiated cells with all the compounds under study except 20,23(OH)₂D₃ (Fig. 10B) when compared to irradiated, ethanol-treated control cells (Fig. 10A, graph on right).

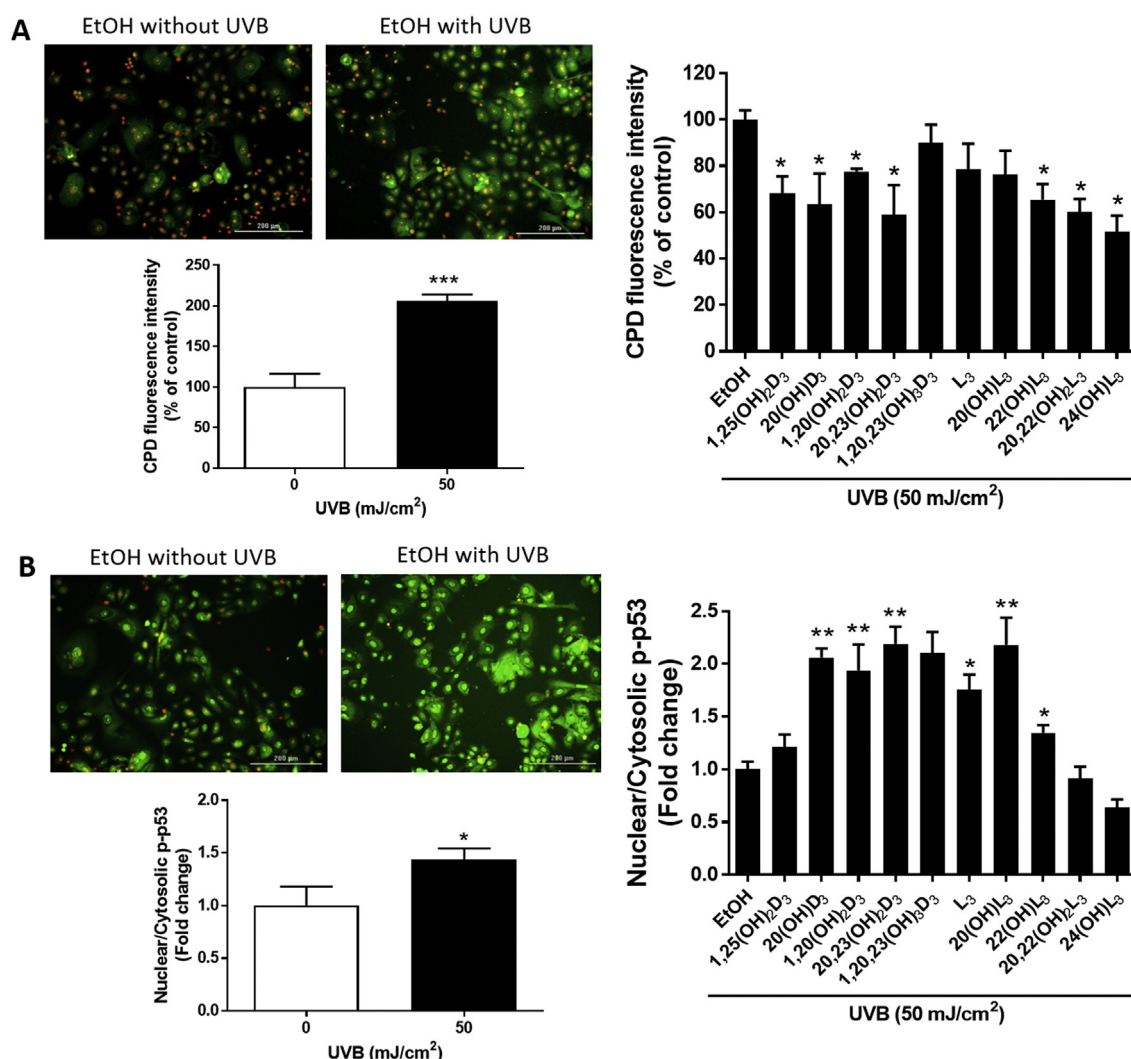


Fig. 5. Novel derivatives of vitamin D₃ and lumisterol reduce levels of CPD and increase levels of phosphorylated p53 in the nucleus of UVB-irradiated cells. Keratinocytes were pretreated with the indicated hydroxy-derivatives of vitamin D₃ or lumisterol (100 nM), or ethanol vehicle, for 24 h before UVB irradiation (50 mJ/cm²). After irradiation, cells were further incubated in fresh media with the same hydroxy-derivative for various times depending on the detection assay. CPD levels (A) were determined at 3 h, while p-p53 levels (B) were determined 1 h post UVB irradiation. Cells were fixed and stained with anti-CPD or anti-phospho-p53 antibody and imaged with a fluorescence microscope, then analysed using the Cytation 5 reader and Graph Pad Prism. Images and graphs on the right show the levels of CPD and p53 in non-irradiated compared with UVB-irradiated (50 mJ/cm²) cells in the absence of the hydroxy-derivatives. Graphs on the right show the fluorescence intensity of irradiated cells treated with the hydroxy-derivatives relative to the ethanol vehicle expressed as a percentage of CPD level and fold change in the nuclear/cytosolic p-p53 ratio. Keratinocytes stained with CPD or p53 antibody exhibited green fluorescence whereas nuclear staining with propidium iodide appears as red fluorescence. Data are presented as (mean ± SD). The statistical significance of differences was evaluated by the student t-test, * P < 0.05, ** P < 0.01, *** P < 0.001 for all conditions.

Nrf2-regulated antioxidant proteins, including catalase (Fig. 11A) and HO-1 (Fig. 11B), significantly increased in cells treated with the hydroxy-derivatives, except for 1,20,23(OH)₃D₃ and 20,22(OH)₂L₃ on HO-1. For MnSOD, only 1,25(OH)₂D₃, 20(OH)D₃, 1,20(OH)₂D₃, 20(OH)L₃ and 20,22(OH)₂L₃ caused a significant increase in its expression following their administration to UV-irradiated cells (Fig. 11C).

Finally, all the vitamin D₃ and lumisterol hydroxy-derivatives tested inhibited the growth of keratinocytes at, at least one of the concentrations tested, when applied after UVB-irradiation of cells (Supplemental Fig. 7).

5. Discussion

Skin is the major barrier between the external environment and the body. The most superficial layer of skin is the epidermis, which contains a large amount of keratinocytes [68,69]. UV irradiation, particularly UVB, causes skin damage and through the induction of DNA damage

can lead to skin carcinogenesis [5,6]. In addition, UVB irradiation also induces ROS formation which then causes oxidative damage to the skin cells [8,70]. Natural as well as synthetic compounds having the ability to reduce excessive free radicals and prevent or reduce DNA damage could potentially be exploited for skin photoprotection [17,50,71–74]. Recently, 1,25(OH)₂D₃ has been shown to protect the skin against oxidative stress [34–36] and to induce DNA damage/repair process [36–38,48] as well as activating Nrf2 expression [34,39].

We have discovered new pathways of vitamin D₃ metabolism initiated by the action of CYP11A1, which have been found to occur in peripheral tissues including the skin [23,27–30,41]. Recent investigations have shown that like 1,25(OH)₂D₃, products of this pathway, 20(OH)D₃ and 20,23(OH)₂D₃, have the ability to protect against ROS formation [47,75,76]. While the protective effects of vitamin D₃ derivatives have been partially investigated, there is a lack of information on the ability of vitamin D₃ derivatives downstream of 20(OH)D₃ or lumisterol or its newly discovered hydroxy-derivatives, to influence

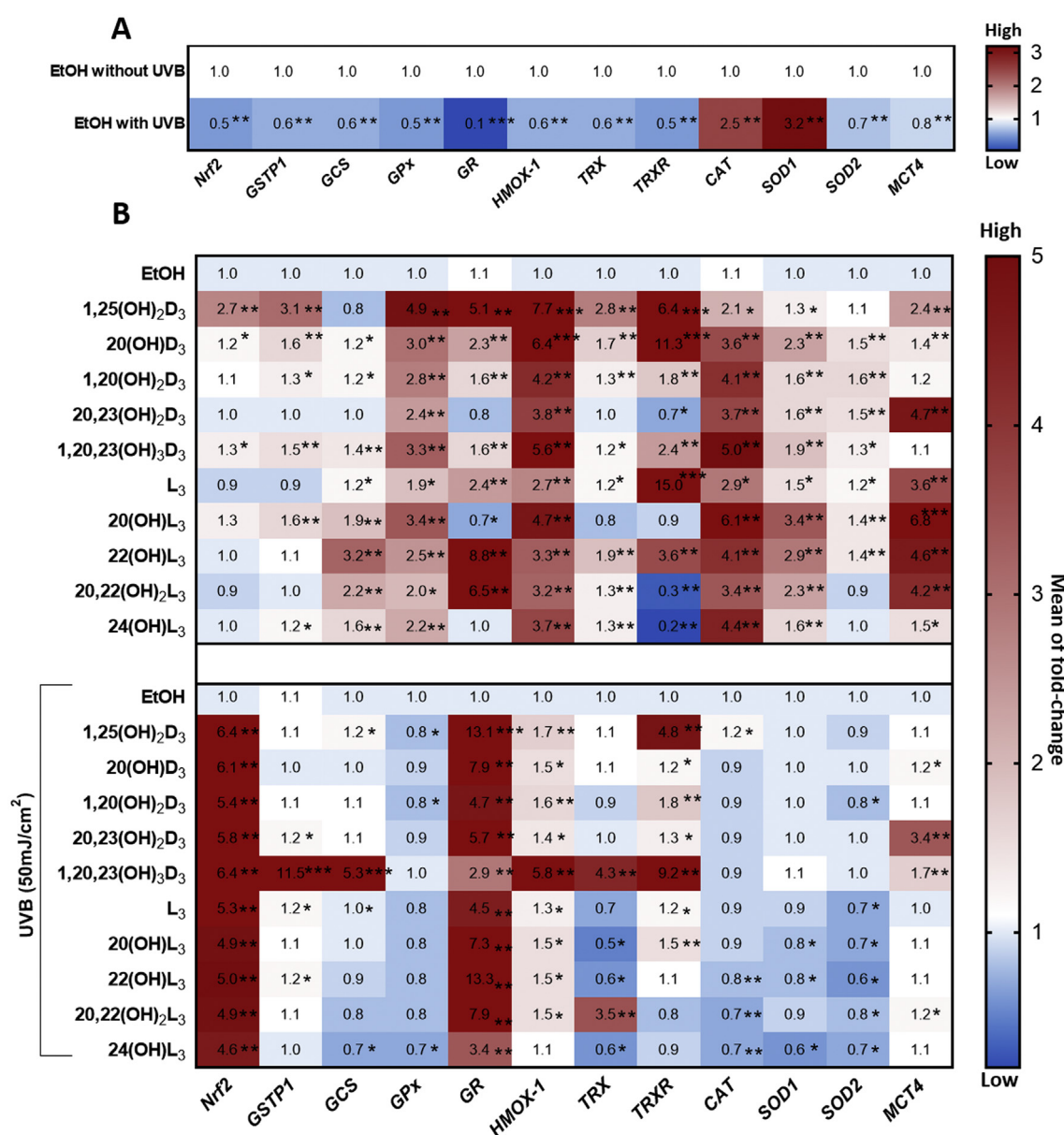


Fig. 6. Heat map summary of the gene expression profile for the antioxidant signaling pathway following the treatment of keratinocytes by novel derivatives of vitamin D₃ or lumisterol. Keratinocytes were pretreated with the indicated hydroxy-derivatives of vitamin D₃ or lumisterol (100 nM), or ethanol vehicle, for 24 h before UVB irradiation (50 mJ/cm²) then further incubated with the same hydroxy-derivative for an additional 24 h. Cells were lysed after treatment and total RNA extracted. Gene expression measurements were confirmed using quantitative real time PCR methods and expression levels normalized the relative to β -actin, cyclophilin, and GAPDH RNA. (A), Heat-maps of log₂ transformed expression ratios for non-irradiated compared with UVB-irradiated (50 mJ/cm²) cells. (B), Irradiated cells pretreated with the hydroxyderivatives (or the ethanol vehicle). Each vertical row represents the same gene product and each horizontal row each sample. The fluorescence range from high (red) to low (blue) is indicated by the colored bar and reflects the degree of fluorescence intensity/gene expression. Data are presented as mean of fold-change (mean \pm SD) calculated from the SYBR fluorescence intensities. The statistical significance of differences was evaluated by the student t-test, * $P < 0.05$, ** $P < 0.01$, *** $P < 0.001$ for all conditions.

ROS levels. We therefore tested a large range of CYP11A1-derived hydroxy-derivatives of vitamin D₃ and lumisterol for their ability to influence oxidant formation. Although most hydroxy-derivatives studied did not significantly inhibit oxidant formation in non-irradiated cells, the same compounds used at the highest concentration (100 nM) caused a marked reduction in the levels of oxidant formation in keratinocytes exposed to UVB. These results indicate that the pretreatment of keratinocytes with CYP11A1-derived vitamin D₃ or lumisterol derivatives protects against cellular damage caused by UV-mediated oxidative stress.

Our previous studies demonstrated the anti-proliferative effects of hydroxy-derivatives of vitamin D₃ [40,41,77] and hydroxylumisterols

on keratinocytes [45]. The current study shows that all of the derivatives tested, which was done at three different concentrations ranging from 1 to 100 nM, showed anti-proliferative effects on keratinocytes exposed to UVB, further emphasizing their photoprotective capabilities. Cell proliferation is regulated by multiple signaling pathways including redox regulation, DNA damage and repair. Redox regulation is important in both the activation of proliferation and arrest of the cell cycle. Redox-sensitive proteins also show the influence on cell cycle progression [78–80]. Some authors reported that the cell proliferation can be promoted by enhancing DNA repair [81,82]. Therefore, some of the modulatory effects on DNA damage and repair under the influence of vitamin D₃ and its derivatives might occur as a function of

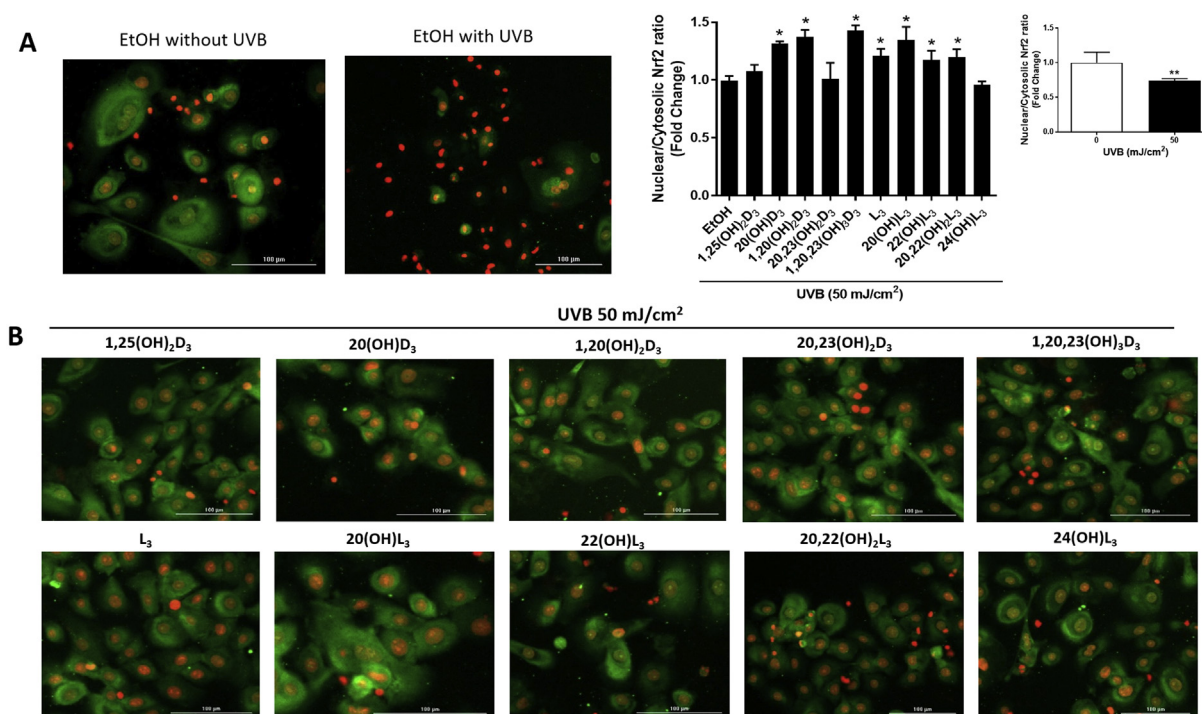


Fig. 7. Novel derivatives of vitamin D₃ and lumisterol stimulate Nrf2 nuclear translocation in UVB-treated keratinocytes. Keratinocytes were pretreated with the indicated hydroxy-derivatives of vitamin D₃ or lumisterol (100 nM), or ethanol vehicle, for 24 h before UVB irradiation (50 mJ/cm²) then further incubated with the same hydroxy-derivative for an additional 24 h. Cells were fixed and stained with anti-Nrf2 antibody and imaged with a fluorescence microscope. Fluorescence intensity was measured using the Cytation 5 reader and data were analysed using Graph Pad Prism. Images and graphs show the levels of fluorescence intensities in non-irradiated compared with UVB-irradiated (50 mJ/cm²) cells (A) and irradiated cells pretreated with the hydroxy-derivatives (B). Keratinocytes stained with Nrf2 antibody exhibited a green fluorescence, while nuclear staining with propidium iodide produced red fluorescence. Data are presented as the nuclear/cytosolic Nrf2 ratio (mean of fold change \pm SD) calculated from fluorescence intensities. The statistical significance of differences was evaluated by the student t-test, * $P < 0.05$, ** $P < 0.01$ for all conditions.

proliferative status rather than induction of stress response pathways.

Our previous results showed that there was a reduction in CPD damage in human keratinocytes treated with 1,25(OH)₂D₃ or 20(OH)D₃ prior to UVB exposure [47]. While the treatment with 1,25(OH)₂D₃ or 20(OH)D₃ reversed the DNA damage by reducing the length of the comet tails [47], the protective effects of other hydroxy-derivatives of 20(OH)D₃ and lumisterol against UVB-induced DNA damage have not been elucidated. In this study we show that other downstream metabolites of 20(OH)D₃, namely 1,20(OH)₂D₃, 20,23(OH)₂D₃, and 1,20,23(OH)₃D₃, and the hydroxylumisterols 20(OH)L₃, 22(OH)L₃, 20,22(OH)₂L₃, and 24(OH)L₃, protect against UVB-induced DNA damage by reducing the comet tail length and CPD formation. Although the CPD levels were not significantly decreased by all the hydroxy-derivatives tested, with 1,20,23(OH)₃D₃, L₃, and 20(OH)L₃ lacking an effect, the others inhibited CPD formation in UVB-irradiated cells. These results indicate that in general the vitamin D₃ and lumisterol hydroxy-derivatives act like 1,25(OH)₂D₃ on DNA repair in keratinocytes exposed to the UVB [36]. The results are also consistent with the reported ability of 20(OH)D₃ to display photoprotective effects when topically applied to murine skin [75].

Following DNA damage, a cellular defense is mounted in order to maintain genomic integrity, including nucleotide excision repair. The 6-4PP photoproduct is repaired only by nucleotide excision repair in human keratinocytes [62,63,83]. A complete repair of 6-4PP was observed in previous studies with synthetic compounds not related to vitamin D₃ [84,85]. 1,25(OH)₂D₃ is also known to protect against DNA damage through the DNA repair system [38]. We thus determined the level of 6-4PP repair in keratinocyte treated with vitamin D₃ and lumisterol hydroxy-derivatives. Most of the compounds under study enhanced the repair of 6-4PPs in UVB-irradiated cells, suggesting that CYP11A1-derived hydroxyderivatives of vitamin D₃ and lumisterol

have the ability to repair UVB-damaged DNA through the DNA repair mechanism described recently for 1,25(OH)₂D₃ [36,38].

Several synthetic compounds that have the ability to scavenge ROS have been reported to activate Nrf2 expression [15,17,50,86,87], while the silencing of Nrf2 in cells significantly reduced the expression of its target antioxidant genes [15]. The lumisterols derivative, 20(OH)L₃, has been shown to induce the expression of several genes involved in anti-oxidative responses [45]. Natural compounds targeting Nrf2 play an important role in the protection against stress-induced skin damage [34,39,57,88–90]. Pre-treatment of cells with 1,25(OH)₂D₃ stimulated translocation of Nrf2 into the nucleus [39], however, other vitamin D₃ derivatives have not been tested previously. We thus investigated whether the vitamin D₃ and lumisterol hydroxy-derivatives we are studying could protect against UVB-induced DNA damage through the modulation of Nrf2. All of these compounds increased Nrf2 levels in the nucleus in UVB-irradiated cells compared to irradiated, ethanol-treated cells. The protective effects of all the hydroxy-derivatives against UVB was further substantiated by their ability to stimulate the expression of genes involved in anti-oxidative stress defense, at the mRNA and protein levels. UVB irradiation impeded the function of Nrf2 by down-regulating Nrf2-antioxidant signaling. Treatment with the hydroxy-derivatives of vitamin D₃ and lumisterol caused significant changes in Nrf2-regulated antioxidant gene expression in cells. Our previous study revealed that UV significantly decreased Nrf2 protein expression, the transcription factor mediating antioxidant responses, 1 h post-irradiation [57]. Two hours post exposure, there was a marked reduction of antioxidant activity for catalase, HO-1, and superoxide dismutase [91]. The immunofluorescence study showed that catalase, HO-1, and superoxide dismutase protein expression were thus detected at 1–3 h post-irradiation. This interesting phenomenon of early detection is in accordance with the previous studies [91–93]. Similarly, UVB-irradiated

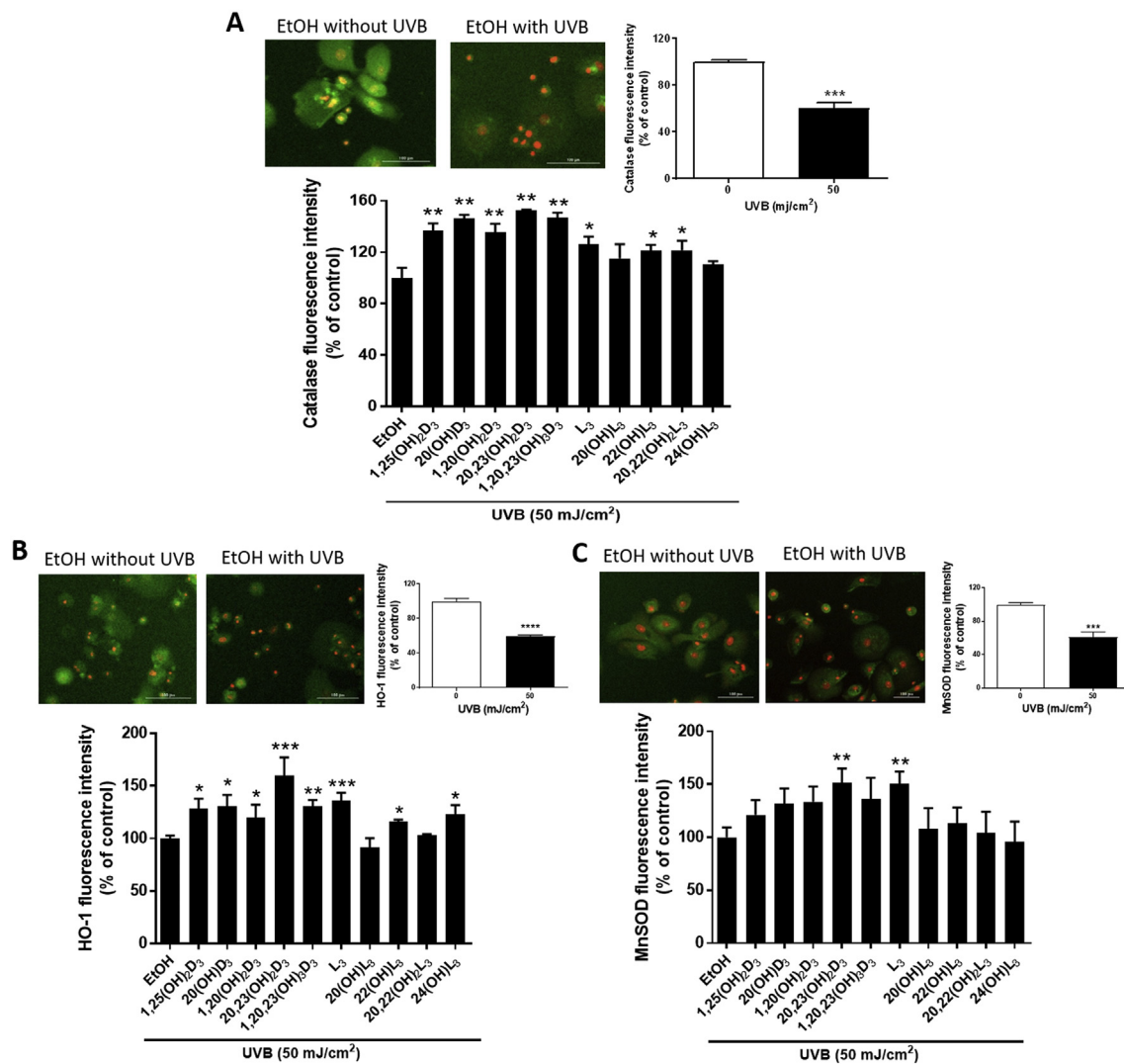


Fig. 8. Novel derivatives of vitamin D₃ and lumisterol elevate members of the Nrf2-regulated antioxidant defense system for UVB-treated keratinocytes. Keratinocytes were pretreated with the indicated hydroxy-derivatives of vitamin D₃ or lumisterol (100 nM), or ethanol vehicle, for 24 h before UVB irradiation (50 mJ/cm²) then further incubated with the same hydroxy-derivative for various times depending on the detection assay. Catalase (CAT) (A) and HO-1 (B) were determined at 3 h, while MnSOD (C) was determined 1 h post UVB irradiation. Cells were fixed and stained with anti-CAT, HO-1, and MnSOD antibody and imaged with a fluorescence microscope. Fluorescence intensity was detected using the Cytation 5 reader and data were analysed using Graph Pad Prism. Images of cells are shown on the upper left for each of A, B and C, and graphs showing the levels of fluorescence intensities in non-irradiated compared with UVB-irradiated cells are upper right. The analysis of the effects of the hydroxy-derivatives relative to the irradiated, ethanol control are shown below the cell images. Keratinocytes stained with CAT, HO-1, and MnSOD antibody exhibited a green fluorescence while nuclear staining with propidium iodide caused red fluorescence. Data are presented as the percentage of control (mean ± SD) calculated from the fluorescence intensities. The statistical significance of differences was evaluated by the student t-test, * P < 0.05, ** P < 0.01, *** P < 0.001 for all conditions.

cells treated with the hydroxyderivatives were able to restore Nrf2 and antioxidant protein levels including CAT and HO-1. Thus, novel CYP11A-derived vitamin D₃ and lumisterol hydroxyderivatives display Nrf2-activating properties correlated with their abilities to stimulate the recovery of keratinocytes from UVB-induced oxidative stress.

The stimulation of the expression of p53 phosphorylated at Ser-15 has been reported for human keratinocytes treated with 1,25(OH)₂D₃ or 20(OH)D₃ prior to UVB exposure [47]. In the current study, we found that most of the vitamin D₃ and lumisterol hydroxy-derivatives tested induced phosphorylated p53 expression using both immuno-fluorescence and nuclear/cytosolic protein expression assays on UVB-irradiated cells. This suggest that the mechanism for photoprotective effects of CYP11A1-derived vitamin D₃ and lumisterol hydroxyderivatives against UVB-induced DNA damage also involves activation of p53, which is in addition to their stimulation of Nrf2 signaling.

The protective effects of natural compounds show a significant

impact on skin in various treatment regimen including pre- and post-treatment [94]. The post-treatment regimen has been used for vitamin D₃ treatment with some diseases including skin protection [95,96]. During the post-treatment, vitamin D₃ reduced the apoptosis and healing process in psoriasis [95]. Additionally, the post-treatment with topical vitamin D₃ has been used in clinical trial as well [96]. Therefore, we found that it is important to test the effect of compounds in protection against UV-induced skin damage when used in both pre-treatment and post-treatment. Following our previous studies on the ability of melatonin to stimulate repair of UVB- damaged DNA when applied after irradiation [15,20], we employed a post-treatment protocol to test whether vitamin D₃ and lumisterol hydroxy-derivatives had similar effects. We found that the addition of most (and in some cases all) of the vitamin D₃ and lumisterol hydroxy-derivatives after UVB exposure increased Nrf2 levels, stimulated the expression of some of its targeted proteins and inhibited the proliferation of UVB-irradiated cells. This

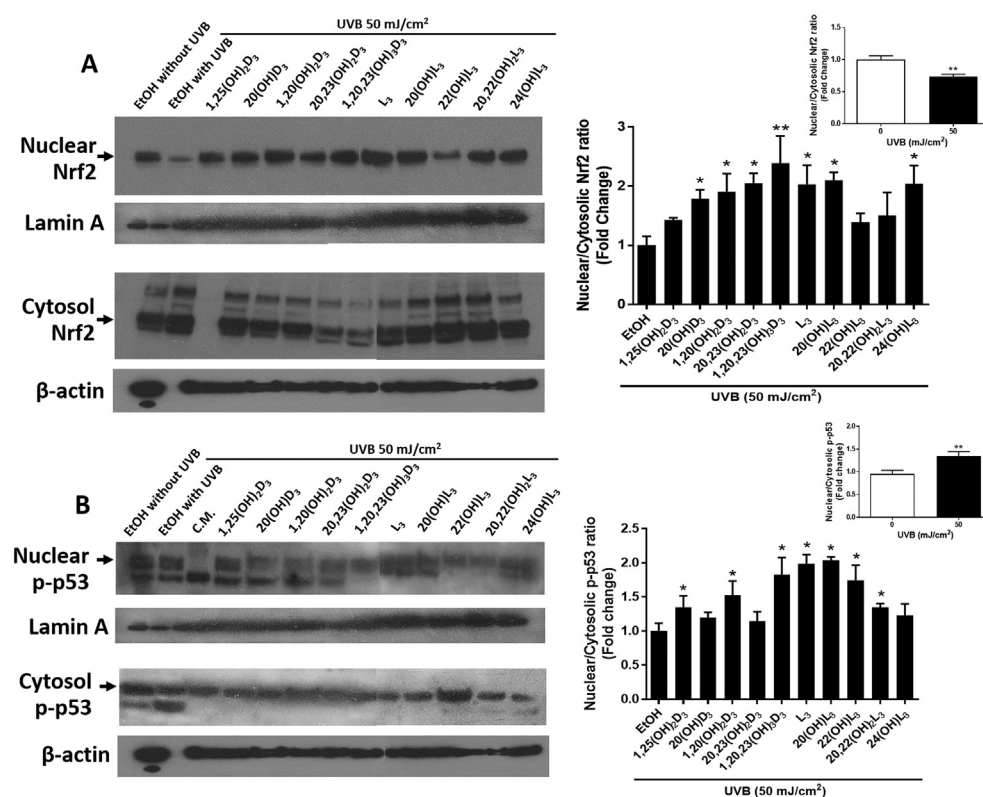


Fig. 9. The vitamin D₃ and lumisterol hydroxy-derivatives increase the level of Nrf2 and phosphorylated p53 protein in the nucleus relative to the cytoplasm. Keratinocytes were pretreated with the indicated hydroxy-derivatives of vitamin D₃ or lumisterol (100 nM), or ethanol vehicle, for 24 h before UVB irradiation (50 mJ/cm²) then further incubated with the same hydroxy-derivative for 24 h. Western blot analysis was performed to determine Nrf2 (A) and phosphorylated p53 (B) levels in nuclear and cytosolic fractions. Nrf2 and phosphor-p53 (Ser15) were detected at approximately 68 and 53 kDa, respectively. Lamin A, the loading control for nuclear protein, was detected at approximately 75 kDa and β-actin, the loading control for cytosolic protein, at 40 kDa. Western blots were analysed by measuring bands intensities in the different lanes using ImageJ software. Graphs on the top right of (A) and (B) show the ratio of nuclear to cytoplasmic protein in UVB-irradiated (50 mJ/cm²) cells compared with non-irradiated cells. Data were calculated from the ratio of Nrf2 or p-p53 band intensities to the loading control, normalized relative to the control (ethanol vehicle or no irradiation). The statistical significance of differences was evaluated by the student t-test, * P < 0.05, ** P < 0.01 for all conditions.

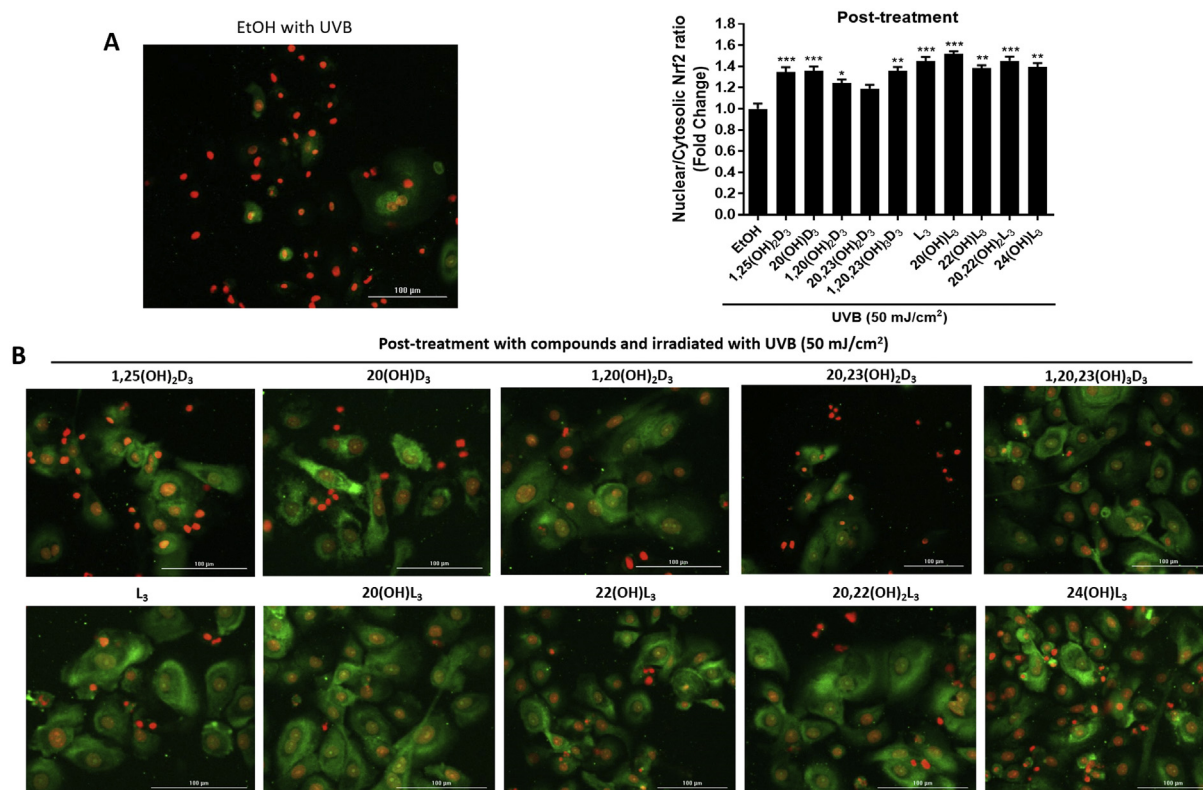


Fig. 10. Effects of post-treatment with novel derivatives of vitamin D₃ and lumisterol on Nrf2 nuclear translocation in human keratinocytes following UVB irradiation. Keratinocytes were exposed to UVB intensities of 50 mJ/cm² and immediately treated with the indicated hydroxy-derivatives of vitamin D₃ or lumisterol (100 nM), or ethanol vehicle, for 24 h. Cells were fixed and stained with anti-Nrf2 antibody and imaged with a fluorescence microscope as in Fig. 7. Keratinocytes stained with Nrf2 antibody exhibited green fluorescence while nuclear staining with propidium iodide caused red fluorescence. (A, top left), Image of ethanol treated, UVB-irradiated control cells. (B), Images of keratinocytes treated with the hydroxy-derivatives after irradiation (below) and Nrf2 levels relative to the ethanol control (top right). Data are presented as nuclear/cytosolic ratio (mean of fold change ± SD) calculated from the fluorescence intensities. The statistical significance of differences was evaluated by the student t-test, * P < 0.05, ** P < 0.01, *** P < 0.001 for all conditions.

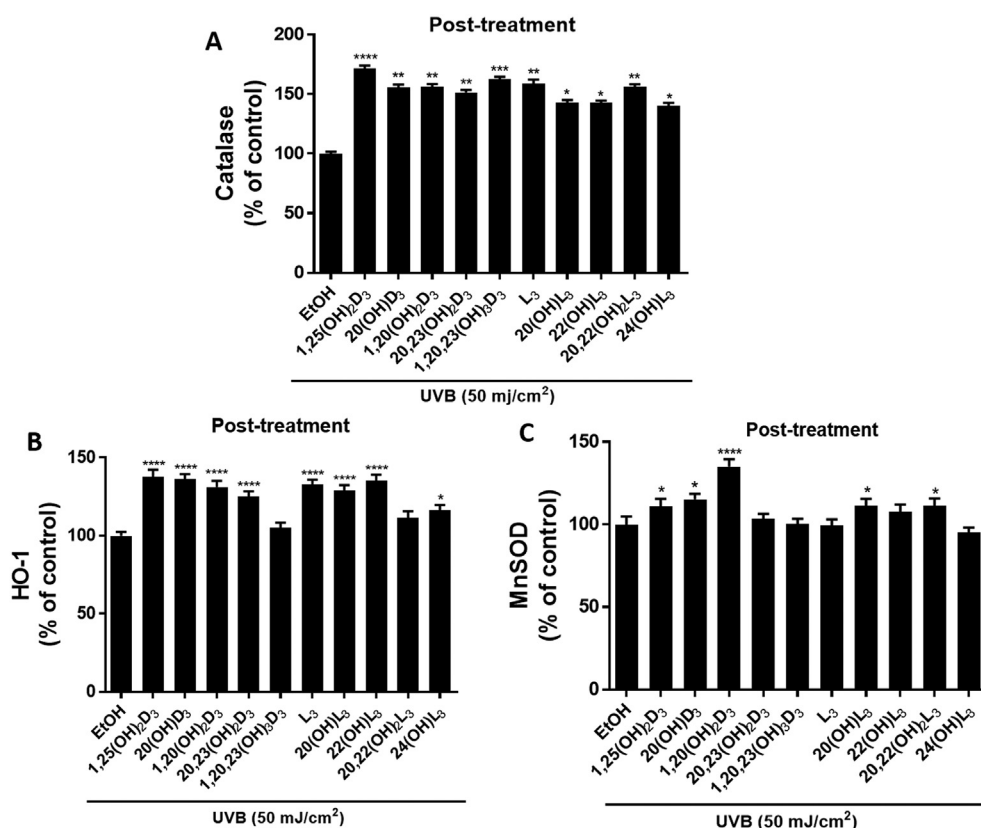


Fig. 11. Effects of post-treatment with novel derivatives of vitamin D₃ and lumisterol on Nrf2 targeted antioxidant proteins following UVB-irradiation. Keratinocytes were exposed to UVB intensities of 50 mJ/cm² and immediately treated with the indicated hydroxy-derivatives of vitamin D₃ or lumisterol (100 nM), or ethanol vehicle, for various times depending on the detection assay. Catalase (CAT) (A) and HO-1 (B) levels were determined at 3 h, while MnSOD (C) was determined 1 h post UVB irradiation. Cells were fixed and stained with anti-CAT, HO-1, or MnSOD antibody, imaged with a fluorescence microscope and analysed using the Cytation 5 reader and Graph Pad Prism. Data are shown as the relative fluorescence intensities of cells treated with the hydroxy-derivatives compared to irradiated, ethanol-treated control cells. Keratinocytes stained with CAT, HO-1, or MnSOD antibody exhibited green fluorescence while nuclear staining with propidium iodine caused red fluorescence. Data are mean \pm SD. The statistical significance of differences was evaluated by the student t-test, * $P < 0.05$, ** $P < 0.01$, *** $P < 0.001$, **** $P < 0.0001$ for all conditions.

indicates that not only pre-treatment but also post-treatment of keratinocytes with the vitamin D₃ and lumisterol hydroxy-derivatives under study can be effective against UVB-induced cell damage. This subject deserves future in-depth detailed testing following protocols described for melatonin treatment [20] in order to define whether these novel vitamin D₃ and lumisterol derivatives are good therapeutic candidates for reversion of skin damage induced by UVB.

The effects of the novel vitamin D₃ and lumisterol derivatives, including the stimulation of the expression of Nrf2-downstream genes and proteins, as well as the photoprotection, are similar to those described for other synthetic and natural compounds including 1,25(OH)₂D₃ [1,15,17,20,36,50,97]. While the role of the vitamin D receptor (VDR) in photoprotection is well established [36,49], the challenge for the future studies is to determine to what degree the VDR versus other nuclear receptors contributes to the photoprotective effects of the novel vitamin D₃ and lumisterol derivatives. It should be noted that retinoic acid orphan receptors (ROR) α and γ and arylhydrocarbon receptor (AhR) can also be activated by some of these compounds [29,45,77,98] and a variation in receptor contribution to the observed effects might explain the lack of activity seen for some derivatives in some assays. In summary, we have defined CYP11A1-derive vitamin D₃ and lumisterol hydroxy-derivatives as protectors against damage induced by UVB, with the potential to repair already existing damage, and we have established the involvement of p53 and Nrf2 in the regulation of these processes.

Epidermal keratinocytes have an indirect effect on the tanning process through the activation of p53-mediated pigment synthesis and the accumulation of melanin in epidermal melanocytes [99]. Furthermore, clinical studies have shown that skin treatments with both oral and topical vitamin D₃ protect against UV-induced inflammation and sunburn [100,101]. In our study we show that vitamin D₃ and its derivatives exhibit protective role against UVB-induced p53 activation, one of biomarkers in the pigmentation mechanism. However, taking into consideration conflicting data on vitamin D effects on melanin

pigmentation [102] or lack of effect of active forms of vitamin D on melanogenesis [103], no direct correlation can be made between tanning and vitamin D action in the human skin. However, it is likely that the photoprotective activity of vitamin D compounds includes a reduction in skin inflammation, which plays a crucial role in sunburn formation [104].

Since our results show the upregulation of Nrf2 activity under the influence of the vitamin D₃ hydroxy-derivatives tested, we plan to investigate in the future whether tested compounds exhibit the protective effects through Nrf2-upstream/downstream signaling [105,106].

6. Conclusion

Data presented here demonstrate that pretreatment of keratinocytes with 1,25(OH)₂D₃, CYP11A1-derived vitamin D₃-hydroxy-derivatives, as well as lumisterol and its hydroxy-derivatives, exert pharmacological protective effects, including free radical scavenging activities against UVB-induced DNA damage and anti-proliferative activities. Additionally, these compounds also protect human keratinocytes against DNA damage through protective pathways that include activation of the Nrf2-antioxidant response and p53-phosphorylation, as well as the induction of DNA repair. Therefore, these compounds can be classified as natural compounds with potent antioxidant properties, targeting Nrf2 and p53 activated pathways to protect the skin from photodamage induced by UVB. Thus, the novel hydroxy-derivatives of vitamin D₃ and lumisterol are promising photoprotective agents and deserve to be further tested using *in vivo* models.

Conflicts of interest

The authors have no conflicts of interest to declare.

Author contributions

A.C. designed and carried out most of the experiments, analysed the data, and wrote the manuscript. Z.J. designed experiments, analysed data and wrote the manuscript. T.K.K. test compounds synthesis, designed experiments. S.G.J. performed DNA Repair analysis and analysed the data. J.A.D. designed experiments and wrote the manuscript. M.F.H. test compounds synthesis and wrote the manuscript. E.K.Y.T. test compounds synthesis. R.C.T. test compounds synthesis, analysed the data and wrote the manuscript. U.P. designed experiments and wrote the manuscript. W.L. test compounds synthesis, read and corrected the manuscript. A.T.S. designed experiments, analysed data and wrote the manuscript.

Acknowledgements

The study was supported by NIH grants 1R01AR073004-01A1 and R01AR071189-01A1 and by a VA merit grant (no. 1I01BX004293-01A1) to ATS, United States.

Appendix A. Supplementary data

Supplementary data to this article can be found online at <https://doi.org/10.1016/j.redox.2019.101206>.

Keratinocytes were pretreated with the indicated vitamin D₃ and lumisterol hydroxy-derivatives for 24 h prior to UV irradiation (50 mJ/cm²). The irradiated cells were further incubated for an additional 4 h with the hydroxy-derivatives or ethanol vehicle, while non-irradiated cells were treated with the ethanol vehicle (comparison presented as insert, top right). Oxidant formation was examined using the DCFDA reagent at 4 h post UVB irradiation. Data are presented as the percentage of the control (mean \pm SD). The statistical significance of differences was evaluated by one-way ANOVA, *P < 0.05, **P < 0.01, ***P < 0.001 for all conditions.

Keratinocytes were pretreated with the indicated hydroxy-derivative of vitamin D₃ or lumisterol (100 nM) for 24 h prior to UV irradiation (200 mJ/cm²), then further incubated with the same hydroxy-derivative for 3 h and subjected to the comet assay. (A), Non-irradiated compared with UVB-irradiated cells without the hydroxy-derivatives; (B) irradiated cells treated with the hydroxy-derivatives. DNA damage was measured as mean tail moment, using Comet score software analysis. Data are presented as the mean tail moment (mean \pm SD). The statistical significance of differences was evaluated by the student t-test, ***P < 0.001 for all conditions.

Keratinocytes were pretreated with the indicated hydroxy-derivatives of vitamin D₃ or lumisterol (100 nM), or ethanol vehicle, for 24 h before UVB irradiation (50 mJ/cm²). After irradiation, cells were further incubated in fresh media with the same hydroxy-derivative for various times depending on the detection assay. CPD levels (A) were determined at 3 h, while p-p53 levels (B) were determined 1 h post UVB irradiation. Cells were fixed and stained with anti-CPD or anti-phospho-p53 antibody and imaged with a fluorescence microscope, then analysed using the Cytation 5 reader and Graph Pad Prism. Images and graphs on the right show the levels of CPD and p53 in non-irradiated compared with UVB-irradiated (50 mJ/cm²) cells in the absence of the hydroxy-derivatives. Graphs on the right show the fluorescence intensity of irradiated cells treated with the hydroxy-derivatives relative to the ethanol vehicle expressed as a percentage of CPD level and fold change in the nuclear/cytosolic p-p53 ratio. Keratinocytes stained with CPD or p53 antibody exhibited green fluorescence whereas nuclear staining with propidium iodine appears as red fluorescence. Data are presented as (mean \pm SD). The statistical significance of differences was evaluated by the student t-test, *P < 0.05, **P < 0.01, ***P < 0.001 for all conditions.

Keratinocytes were pretreated with the indicated hydroxy-derivatives of vitamin D₃ or lumisterol (100 nM), or ethanol vehicle, for 24 h

before UVB irradiation (50 mJ/cm²) then further incubated with the same hydroxy-derivative for an additional 24 h. Cells were lysed after treatment and total RNA extracted. Gene expression measurements were confirmed using quantitative real time PCR methods and expression levels normalized the relative to β -actin, cyclophilin, and GAPDH RNA. (A), Heat-maps of log 2 transformed expression ratios for non-irradiated compared with UVB-irradiated (50 mJ/cm²) cells. (B), Irradiated cells pretreated with the hydroxyderivatives (or the ethanol vehicle). Each vertical row represents the same gene product and each horizontal row each sample. The fluorescence range from high (red) to low (blue) is indicated by the colored bar and reflects the degree of fluorescence intensity/gene expression. Data are presented as mean of fold-change (mean \pm SD) calculated from the SYBR fluorescence intensities. The statistical significance of differences was evaluated by the student t-test, *P < 0.05, **P < 0.01, ***P < 0.001 for all conditions.

Keratinocytes were pretreated with the indicated hydroxy-derivatives of vitamin D₃ or lumisterol (100 nM), or ethanol vehicle, for 24 h before UVB irradiation (50 mJ/cm²) then further incubated with the same hydroxy-derivative for an additional 24 h. Cells were fixed and stained with anti-Nrf2 antibody and imaged with a fluorescence microscope. Fluorescence intensity was measured using the Cytation 5 reader and data were analysed using Graph Pad Prism. Images and graphs show the levels of fluorescence intensities in non-irradiated compared with UVB-irradiated (50 mJ/cm²) cells (A) and irradiated cells pretreated with the hydroxy-derivatives (B). Keratinocytes stained with Nrf2 antibody exhibited a green fluorescence, while nuclear staining with propidium iodine produced red fluorescence. Data are presented as the nuclear/cytosolic Nrf2 ratio (mean of fold change \pm SD) calculated from fluorescence intensities. The statistical significance of differences was evaluated by the student t-test, *P < 0.05, **P < 0.01 for all conditions.

Keratinocytes were pretreated with the indicated hydroxy-derivatives of vitamin D₃ or lumisterol (100 nM), or ethanol vehicle, for 24 h before UVB irradiation (50 mJ/cm²) then further incubated with the same hydroxy-derivative for various times depending on the detection assay. Catalase (CAT) (A) and HO-1 (B) were determined at 3 h, while MnSOD (C) was determined 1 h post UVB irradiation. Cells were fixed and stained with anti-CAT, HO-1, and MnSOD antibody and imaged with a fluorescence microscope. Fluorescence intensity was detected using the Cytation 5 reader and data were analysed using Graph Pad Prism. Images of cells are shown on the upper left for each of A, B and C, and graphs showing the levels of fluorescence intensities in non-irradiated compared with UVB-irradiated cells are upper right. The analysis of the effects of the hydroxy-derivatives relative to the irradiated, ethanol control are shown below the cell images. Keratinocytes stained with CAT, HO-1, and MnSOD antibody exhibited a green fluorescence while nuclear staining with propidium iodine caused red fluorescence. Data are presented as the percentage of control (mean \pm SD) calculated from the fluorescence intensities. The statistical significance of differences was evaluated by the student t-test, *P < 0.05, **P < 0.01, ***P < 0.001 for all conditions.

Keratinocytes were pretreated with the indicated hydroxy-derivatives of vitamin D₃ or lumisterol (100 nM), or ethanol vehicle, for 24 h before UVB irradiation (50 mJ/cm²) then further incubated with the same hydroxy-derivative for 24 h. Western blot analysis was performed to determine Nrf2 (A) and phosphorylated p53 (B) levels in nuclear and cytosolic fractions. Nrf2 and phosphor-p53 (Ser15) were detected at approximately 68 and 53 kDa, respectively. Lamin A, the loading control for nuclear protein, was detected at approximately 75 kDa and β -actin, the loading control for cytosolic protein, at 40 kDa. Western blots were analysed by measuring bands intensities in the different lanes using ImageJ software. Graphs on the top right of (A) and (B) show the ratio of nuclear to cytoplasmic protein in UVB-irradiated (50 mJ/cm²) cells compared with non-irradiated cells. Data were calculated from the ratio of Nrf2 or p-p53 band intensities to the loading control,

normalized relative to the control (ethanol vehicle or no irradiation). The statistical significance of differences was evaluated by the student t-test, * $P < 0.05$, ** $P < 0.01$ for all conditions.

Keratinocytes were exposed to UVB intensities of 50 mJ/cm² and immediately treated with the indicated hydroxy-derivatives of vitamin D₃ or lumisterol (100 nM), or ethanol vehicle, for 24 h.

Cells were fixed and stained with anti-Nrf2 antibody and imaged with a fluorescence microscope as in Fig. 7. Keratinocytes stained with Nrf2 antibody exhibited green fluorescence while nuclear staining with propidium iodine caused red fluorescence. (A, top left), Image of ethanol treated, UVB-irradiated control cells. (B), Images of keratinocytes treated with the hydroxy-derivatives after irradiation (below) and Nrf2 levels relative to the ethanol control (top right). Data are presented as nuclear/cytosolic ratio (mean of fold change \pm SD) calculated from the fluorescence intensities. The statistical significance of differences was evaluated by the student t-test, * $P < 0.05$, ** $P < 0.01$, *** $P < 0.001$ for all conditions.

Keratinocytes were exposed to UVB intensities of 50 mJ/cm² and immediately treated with the indicated hydroxy-derivatives of vitamin D₃ or lumisterol (100 nM), or ethanol vehicle, for various times depending on the detection assay. Catalase (CAT) (A) and HO-1 (B) levels were determined at 3 h, while MnSOD (C) was determined 1 h post UVB irradiation. Cells were fixed and stained with anti-CAT, HO-1, or MnSOD antibody, imaged with a fluorescence microscope and analysed using the Cytation 5 reader and Graph Pad Prism. Data are shown as the relative fluorescence intensities of cells treated with the hydroxy-derivatives compared to irradiated, ethanol-treated control cells. Keratinocytes stained with CAT, HO-1, or MnSOD antibody exhibited green fluorescence while nuclear staining with propidium iodine caused red fluorescence. Data are mean \pm SD. The statistical significance of differences was evaluated by the student t-test, * $P < 0.05$, ** $P < 0.01$, *** $P < 0.001$, **** $P < 0.0001$ for all conditions.

References

- [1] S. Tao, S.L. Park, M. Rojo de la Vega, D.D. Zhang, G.T. Wondrak, Systemic administration of the apocarotenoid bixin protects skin against solar UV-induced damage through activation of NRF2, *Free Radic. Biol. Med.* 89 (2015) 690–700.
- [2] G.T. Wondrak, M.J. Roberts, M.K. Jacobson, E.L. Jacobson, 3-hydroxypyridine chromophores are endogenous sensitizers of photooxidative stress in human skin cells, *J. Biol. Chem.* 279 (29) (2004) 30009–30020.
- [3] H.L. Lo, S. Nakajima, L. Ma, B. Walter, A. Yasui, D.W. Ethell, et al., Differential biologic effects of CPD and 6-4PP UV-induced DNA damage on the induction of apoptosis and cell-cycle arrest, *BMC Cancer* 5 (2005) 135.
- [4] U. Panich, G. Sittithumcharee, N. Rathviboon, S. Jirawatnotai, Ultraviolet radiation-induced skin aging: the role of DNA damage and oxidative stress in epidermal stem cell damage mediated skin aging, *Stem Cell. Int.* 2016 (2016) 7370642.
- [5] H. Raad, M. Serrano-Sanchez, G. Harfouche, W. Mahfouf, D. Bortolotto, V. Bergeron, et al., NADPH oxidase-1 plays a key role in keratinocyte responses to UV radiation and UVB-induced skin carcinogenesis, *J. Investig. Dermatol.* 137 (6) (2017) 1311–1321.
- [6] S. Jeayeng, A. Wongkajornsilp, A.T. Slominski, S. Jirawatnotai, S. Sampattavanich, U. Panich, Nrf2 in keratinocytes modulates UVB-induced DNA damage and apoptosis in melanocytes through MAPK signaling, *Free Radic. Biol. Med.* 108 (2017) 918–928.
- [7] S. Roy, G. Deep, C. Agarwal, R. Agarwal, Silibinin prevents ultraviolet B radiation-induced epidermal damages in JB6 cells and mouse skin in a p53-GADD45alpha-dependent manner, *Carcinogenesis* 33 (3) (2012) 629–636.
- [8] M.C. Drigeard Desgarnier, P.J. Rochette, Enhancement of UVB-induced DNA damage repair after a chronic low-dose UVB pre-stimulation, *DNA Repair (Amst)* 63 (2018) 56–62.
- [9] A.R. Nunes, I.G.P. Vieira, D.B. Queiroz, A. Leal, S. Maia Morais, D.F. Muniz, et al., Use of flavonoids and cinnamates, the main photoprotectors with natural origin, *Adv. Pharmacol. Sci.* 2018 (2018) 5341487.
- [10] H.Y. Kim, S.K. Sah, S.S. Choi, T.Y. Kim, Inhibitory effects of extracellular superoxide dismutase on ultraviolet B-induced melanogenesis in murine skin and melanocytes, *Life Sci.* 210 (2018) 201–208.
- [11] A.R. Nunes, A.L.M. Rodrigues, D.B. de Queiroz, I.G.P. Vieira, J.F.C. Neto, J.T.C. Junior, et al., Photoprotective potential of medicinal plants from Cerrado biome (Brazil) in relation to phenolic content and antioxidant activity, *J. Photochem. Photobiol., B* 189 (2018) 119–123.
- [12] A.T. Slominski, M.A. Zmijewski, P.M. Plonka, J.P. Szaflarski, R. Paus, How UV light touches the brain and endocrine system through skin, and why, *Endocrinology* 159 (5) (2018) 1992–2007.
- [13] H. Ikehata, M. Yamamoto, Roles of the KEAP1-NRF2 system in mammalian skin exposed to UV radiation, *Toxicol. Appl. Pharmacol.* 360 (2018) 69–77.
- [14] Q. Ma, Role of nrf2 in oxidative stress and toxicity, *Annu. Rev. Pharmacol. Toxicol.* 53 (2013) 401–426.
- [15] Z. Janjetovic, S.G. Jarrett, E.F. Lee, C. Duprey, R.J. Reiter, A.T. Slominski, Melatonin and its metabolites protect human melanocytes against UVB-induced damage: involvement of NRF2-mediated pathways, *Sci. Rep.* 7 (1) (2017) 1274.
- [16] G. Chhabra, D.R. Garvey, C.K. Singh, C.A. Mintie, N. Ahmad, Effects and mechanism of nicotinamide against UVA- and/or UVB-mediated DNA damages in normal melanocytes, *Photochem. Photobiol.* 95 (1) (2019) 331–337.
- [17] M. Rojo de la Vega, D.D. Zhang, G.T. Wondrak, Topical bixin confers NRF2-dependent protection against photodamage and hair graying in mouse skin, *Front. Pharmacol.* 9 (2018) 287.
- [18] A. Gegotek, A. Jastrzab, I. Jarocka-Karpowicz, M. Muszynska, E. Skrzydlewska, The effect of sea buckthorn (hippophae rhamnoides L.) seed oil on UV-induced changes in lipid metabolism of human skin cells, *Antioxidants (Basel)* 7 (9) (2018).
- [19] M. Kim, Y.G. Park, H.J. Lee, S.J. Lim, C.W. Nho, Younginsides A and C isolated from youngia denticulatum inhibit UVB-induced MMP expression and promote type I procollagen production via repression of MAPK/AP-1/NF-kappaB and activation of AMPK/Nrf2 in HaCaT cells and human dermal fibroblasts, *J. Agric. Food Chem.* 63 (22) (2015) 5428–5438.
- [20] C. Skobowiat, A.A. Brozyna, Z. Janjetovic, S. Jeayeng, A.S.W. Oak, T.K. Kim, et al., Melatonin and its derivatives counteract the ultraviolet B radiation-induced damage in human and porcine skin ex vivo, *J. Pineal Res.* 65 (2) (2018) e12501.
- [21] M.F. Holick, M.B. Clark, The photobiogenesis and metabolism of vitamin D, *Fed. Proc.* 37 (12) (1978) 2567–2574.
- [22] M.F. Holick, Vitamin D: a millennium perspective, *J. Cell. Biochem.* 88 (2) (2003) 296–307.
- [23] R.C. Tuckey, C.Y.S. Cheng, A.T. Slominski, The serum vitamin D metabolome: what we know and what is still to discover, *J. Steroid Biochem. Mol. Biol.* 186 (2019) 4–21.
- [24] G. Jones, D.E. Prosser, M. Kaufmann, Cytochrome P450-mediated metabolism of vitamin D, *J. Lipid Res.* 55 (1) (2014) 13–31.
- [25] D.D. Bikle, Vitamin D metabolism, mechanism of action, and clinical applications, *Chem. Biol.* 21 (3) (2014) 319–329.
- [26] R.C. Tuckey, W. Li, D. Ma, C.Y.S. Cheng, K.M. Wang, T.K. Kim, et al., CYP27A1 acts on the pre-vitamin D3 photoproduct, lumisterol, producing biologically active hydroxy-metabolites, *J. Steroid Biochem. Mol. Biol.* 181 (2018) 1–10.
- [27] A. Slominski, T.K. Kim, M.A. Zmijewski, Z. Janjetovic, W. Li, J. Chen, et al., Novel vitamin D photoproducts and their precursors in the skin, *Dermatoendocrinol* 5 (1) (2013) 7–19.
- [28] A.T. Slominski, A.A. Brozyna, M.A. Zmijewski, W. Jozwicki, A.M. Jetten, R.S. Mason, et al., Vitamin D signaling and melanoma: role of vitamin D and its receptors in melanoma progression and management, *Lab. Invest.* 97 (6) (2017) 706–724.
- [29] A.T. Slominski, T.K. Kim, Z. Janjetovic, A.A. Brozyna, M.A. Zmijewski, H. Xu, et al., Differential and overlapping effects of 20,23(OH)(2)D3 and 1,25(OH)(2)D3 on gene expression in human epidermal keratinocytes: identification of AhR as an alternative receptor for 20,23(OH)(2)D3, *Int. J. Mol. Sci.* 19 (10) (2018).
- [30] A.T. Slominski, T.K. Kim, W. Li, A. Postlethwaite, E.W. Tieu, E.K. Tang, et al., Detection of novel CYP11A1-derived secosteroids in the human epidermis and serum and pig adrenal gland, *Sci. Rep.* 5 (2015) 14875.
- [31] R.C. Tuckey, W. Li, J.K. Zjawiony, M.A. Zmijewski, M.N. Nguyen, T. Sweatman, et al., Pathways and products for the metabolism of vitamin D3 by cytochrome P450scc, *FEBS J.* 275 (10) (2008) 2585–2596.
- [32] A. Slominski, I. Semak, J. Zjawiony, J. Wortsman, W. Li, A. Szczesniowski, et al., The cytochrome P450scc system opens an alternate pathway of vitamin D3 metabolism, *FEBS J.* 272 (16) (2005) 4080–4090.
- [33] A.T. Slominski, T.K. Kim, H.Z. Shehabi, I. Semak, E.K. Tang, M.N. Nguyen, et al., In vivo evidence for a novel pathway of vitamin D(3) metabolism initiated by P450scc and modified by CYP27B1, *FASEB J. Offic. Publ. Fed. Am. Soc. Exp. Biol.* 26 (9) (2012) 3901–3915.
- [34] T.M. Teixeira, D.C. da Costa, A.C. Resende, C.O. Soulage, F.F. Bezerra, J.B. Daleprane, Activation of nrf2-antioxidant signaling by 1,25-dihydroxycholecalciferol prevents leptin-induced oxidative stress and inflammation in human endothelial cells, *J. Nutr.* 147 (4) (2017) 506–513.
- [35] P. Manna, A.E. Achari, S.K. Jain, Vitamin D supplementation inhibits oxidative stress and upregulate SIRT1/AMPK/GLUT4 cascade in high glucose-treated 3T3L1 adipocytes and in adipose tissue of high fat diet-fed diabetic mice, *Arch. Biochem. Biophys.* 615 (2017) 22–34.
- [36] M.S. Rybchyn, W.G.M. De Silva, V.B. Sequeira, B.Y. McCarthy, A.V. Dilley, K.M. Dixon, et al., Enhanced repair of UV-induced DNA damage by 1,25-dihydroxyvitamin D3 in skin is linked to pathways that control cellular energy, *J. Investig. Dermatol.* 138 (5) (2018) 1146–1156.
- [37] S.E. Judd, S.N. Raiser, M. Kumari, V. Tangpricha, 1,25-dihydroxyvitamin D3 reduces systolic blood pressure in hypertensive adults: a pilot feasibility study, *J. Steroid Biochem. Mol. Biol.* 121 (1–2) (2010) 445–447.
- [38] L. Tremezaygues, M. Seifert, T. Vogt, W. Tilgen, J. Reichrath, 1,25-dihydroxyvitamin D3 modulates effects of ionizing radiation (IR) on human keratinocytes: in vitro analysis of cell viability/proliferation, DNA-damage and -repair, *J. Steroid Biochem. Mol. Biol.* 121 (1–2) (2010) 324–327.
- [39] Z. Rao, N. Zhang, N. Xu, Y. Pan, M. Xiao, J. Wu, et al., 1,25-Dihydroxyvitamin D inhibits LPS-induced high-mobility group box 1 (HMGB1) secretion via targeting the NF-E2-Related factor 2-hemeoxygenase-1-HMGB1 pathway in macrophages, *Front. Immunol.* 8 (2017) 1308.
- [40] B. Zbyetk, Z. Janjetovic, R.C. Tuckey, M.A. Zmijewski, T.W. Sweatman, E. Jones, et al., 20-Hydroxyvitamin D3, a product of vitamin D3 hydroxylation by

- cytochrome P450scc, stimulates keratinocyte differentiation, *J. Investig. Dermatol.* 128 (9) (2008) 2271–2280.
- [41] A.T. Slominski, T.K. Kim, W. Li, A.K. Yi, A. Postlethwaite, R.C. Tuckey, The role of CYP11A1 in the production of vitamin D metabolites and their role in the regulation of epidermal functions, *J. Steroid Biochem. Mol. Biol.* 144 Pt (A) (2014) 28–39.
 - [42] Z. Janjetovic, R.C. Tuckey, M.N. Nguyen, E.M. Thorpe Jr., Slominski AT. 20,23-dihydroxyvitamin D₃, novel P450scc product, stimulates differentiation and inhibits proliferation and NF-kappaB activity in human keratinocytes, *J. Cell. Physiol.* 223 (1) (2010) 36–48.
 - [43] R.C. Tuckey, A.T. Slominski, C.Y. Cheng, J. Chen, T.K. Kim, M. Xiao, et al., Lumisterol is metabolized by CYP11A1: discovery of a new pathway, *Int. J. Biochem. Cell Biol.* 55 (2014) 24–34.
 - [44] A.T. Slominski, W. Li, T.K. Kim, I. Semak, J. Wang, J.K. Zjawiony, et al., Novel activities of CYP11A1 and their potential physiological significance, *J. Steroid Biochem. Mol. Biol.* 151 (2015) 25–37.
 - [45] A.T. Slominski, T.K. Kim, J.V. Hobarth, Z. Janjetovic, A.S.W. Oak, A. Postlethwaite, et al., Characterization of a new pathway that activates lumisterol in vivo to biologically active hydroxylumisterols, *Sci. Rep.* 7 (1) (2017) 11434.
 - [46] L. Hu, D.D. Bikle, Y. Oda, Reciprocal role of vitamin D receptor on beta-catenin regulated keratinocyte proliferation and differentiation, *J. Steroid Biochem. Mol. Biol.* 144 Pt (A) (2014) 237–241.
 - [47] A.T. Slominski, Z. Janjetovic, T.K. Kim, P. Wasilewski, S. Rosas, S. Hanna, et al., Novel non-calcemic secosteroids that are produced by human epidermal keratinocytes protect against solar radiation, *J. Steroid Biochem. Mol. Biol.* 148 (2015) 52–63.
 - [48] E.J. Song, C. Gordon-Thomson, L. Cole, H. Stern, G.M. Halliday, D.L. Damian, et al., 1alpha,25-Dihydroxyvitamin D₃ reduces several types of UV-induced DNA damage and contributes to photoprotection, *J. Steroid Biochem. Mol. Biol.* 136 (2013) 131–138.
 - [49] D.D. Bikle, Vitamin D receptor, a tumor suppressor in skin, *Can. J. Physiol. Pharmacol.* 93 (5) (2015) 349–354.
 - [50] M. Rojo de la Vega, A. Krajisnik, D.D. Zhang, G.T. Wondrak, Targeting NRF2 for improved skin barrier function and photoprotection: focus on the achiote-derived apocarotenoid bixin, *Nutrients* 9 (12) (2017).
 - [51] R.C. Tuckey, W. Li, H.Z. Shehaby, Z. Janjetovic, M.N. Nguyen, T.K. Kim, et al., Production of 22-hydroxy metabolites of vitamin D₃ by cytochrome p450scc (CYP11A1) and analysis of their biological activities on skin cells, *Drug Metab. Dispos.* 39 (9) (2011) 1577–1588.
 - [52] W. Li, J. Chen, Z. Janjetovic, T.K. Kim, T. Sweatman, Y. Lu, et al., Chemical synthesis of 20S-hydroxyvitamin D₃, which shows antiproliferative activity, *Steroids* 75 (12) (2010) 926–935.
 - [53] J. Chen, J. Wang, T.K. Kim, E.W. Tieu, E.K. Tang, Z. Lin, et al., Novel vitamin D analogs as potential therapeutics: metabolism, toxicity profiling, and anti-proliferative activity, *Anticancer Res.* 34 (5) (2014) 2153–2163.
 - [54] Z. Janjetovic, M.A. Zmijewski, R.C. Tuckey, D.A. DeLeon, M.N. Nguyen, L.M. Pfeffer, et al., 20-Hydroxycholecalciferol, product of vitamin D₃ hydroxylation by P450scc, decreases NF-kappaB activity by increasing IkappaB alpha levels in human keratinocytes, *PLoS One* 4 (6) (2009) e5988.
 - [55] S.G. Jarrett, M. Novak, S. Dabernat, J.Y. Daniel, I. Mellon, Q. Zhang, et al., Metastasis suppressor NM23-H1 promotes repair of UV-induced DNA damage and suppresses UV-induced melanomagenesis, *Cancer Res.* 72 (1) (2012) 133–143.
 - [56] S.G. Jarrett, K.M. Carter, B.J. Shelton, J.A. D'Orazio, The melanocortin signaling cAMP axis accelerates repair and reduces mutagenesis of platinum-induced DNA damage, *Sci. Rep.* 7 (1) (2017) 11708.
 - [57] A. Chaiprasongsuk, J. Lohakul, K. Soontrapa, S. Sampattavanich, P. Akarasereenont, U. Panich, Activation of Nrf2 reduces UVA-mediated MMP-1 upregulation via MAPK/AP-1 signaling cascades: the photoprotective effects of sulforaphane and hispidulin, *J. Pharmacol. Exp. Ther.* 360 (3) (2017) 388–398.
 - [58] M. Noursadeghi, J. Tsang, T. Hausteiner, R.F. Miller, B.M. Chain, D.R. Katz, Quantitative imaging assay for NF-kappaB nuclear translocation in primary human macrophages, *J. Immunol. Methods* 329 (1–2) (2008) 194–200.
 - [59] C. Skobowiat, A.S. Oak, T.K. Kim, C.H. Yang, L.M. Pfeffer, R.C. Tuckey, et al., Noncalcemic 20-hydroxyvitamin D₃ inhibits human melanoma growth in vitro and in vivo models, *Oncotarget* 8 (6) (2017) 9823–9834.
 - [60] M.N. Ombra, P. Paliogiannis, V. Doneddu, M.C. Sini, M. Colombino, C. Rozzo, et al., Vitamin D status and risk for malignant cutaneous melanoma: recent advances, *Eur. J. Cancer Prev.* 26 (6) (2017) 532–541.
 - [61] S.D. Lamore, C.M. Cabello, G.T. Wondrak, The topical antimicrobial zinc pyrithione is a heat shock response inducer that causes DNA damage and PARP-dependent energy crisis in human skin cells, *Cell Stress Chaperones* 15 (3) (2010) 309–322.
 - [62] J.M. Lee, J.M. Park, T.H. Kang, Enhancement of UV-induced nucleotide excision repair activity upon forskolin treatment is cell growth-dependent, *BMB Rep.* 49 (10) (2016) 566–571.
 - [63] S. Katsumi, N. Kobayashi, K. Imoto, A. Nakagawa, Y. Yamashina, T. Muramatsu, et al., In situ visualization of ultraviolet-light-induced DNA damage repair in locally irradiated human fibroblasts, *J. Investig. Dermatol.* 117 (5) (2001) 1156–1161.
 - [64] M. Dreze, A.S. Calkins, J. Galiczka, D.J. Echelman, M.R. Schnorenberg, G.L. Fell, et al., Monitoring repair of UV-induced 6-4-photoproducts with a purified DDB2 protein complex, *PLoS One* 9 (1) (2014) e85896.
 - [65] A. Gegotek, E. Skrzydlewska, The role of transcription factor Nrf2 in skin cells metabolism, *Arch. Dermatol. Res.* 307 (5) (2015) 385–396.
 - [66] K. Diehl, L.A. Dinges, O. Helm, N. Ammar, D. Plundrich, A. Arlt, et al., Nuclear factor E2-related factor-2 has a differential impact on MCT1 and MCT4 lactate carrier expression in colonic epithelial cells: a condition favoring metabolic symbiosis between colorectal cancer and stromal cells, *Oncogene* 37 (1) (2018) 39–51.
 - [67] A.I. Potapovich, V.A. Kostyuk, T.V. Kostyuk, C. de Luca, L.G. Korkina, Effects of pre- and post-treatment with plant polyphenols on human keratinocyte responses to solar UV, *Inflamm. Res.* 62 (8) (2013) 773–780.
 - [68] H. Tsuruoka, W. Khovidhunkit, B.E. Brown, J.W. Fluhr, P.M. Elias, K.R. Feingold, Scavenger receptor class B type I is expressed in cultured keratinocytes and epidermis. Regulation in response to changes in cholesterol homeostasis and barrier requirements, *J. Biol. Chem.* 277 (4) (2002) 2916–2922.
 - [69] A.T. Slominski, M.A. Zmijewski, C. Skobowiat, B. Zbytek, R.M. Slominski, J.D. Steketee, Sensing the environment: regulation of local and global homeostasis by the skin's neuroendocrine system, *Adv. Anat. Embryol. Cell Biol.* 212 (2012) 1–115 v, vii.
 - [70] D. Bennet, S. Kim, Evaluation of UV radiation-induced toxicity and biophysical changes in various skin cells with photo-shielding molecules, *Analyst* 140 (18) (2015) 6343–6353.
 - [71] A.A. Farooqi, R.N. Li, H.W. Huang, M. Ismail, S.S. Yuan, H.M. Wang, et al., Natural products mediated regulation of oxidative stress and DNA damage in ultraviolet exposed skin cells, *Curr. Pharmaceut. Biotechnol.* 16 (12) (2015) 1078–1084.
 - [72] U. Golla, S.S. Bhimathathi, Evaluation of antioxidant and DNA damage protection activity of the hydroalcoholic extract of *Desmostachya bipinnata* L. Stapf, *Sci. World J.* 2014 (2014) 215084.
 - [73] G. Petruk, R. Del Giudice, M.M. Rigano, D.M. Monti, Antioxidants from plants protect against skin photoaging, *Oxid. Med. Cell Longev.* 2018 (2018) 1454936.
 - [74] G. Petruk, A. Raiola, R. Del Giudice, A. Barone, L. Frusciante, M.M. Rigano, et al., An ascorbic acid-enriched tomato genotype to fight UVA-induced oxidative stress in normal human keratinocytes, *J. Photochem. Photobiol., B* 163 (2016) 284–289.
 - [75] W. Tongkao-On, S. Carter, V.E. Reeve, K.M. Dixon, C. Gordon-Thomson, G.M. Halliday, et al., CYP11A1 in skin: an alternative route to photoprotection by vitamin D compounds, *J. Steroid Biochem. Mol. Biol.* 148 (2015) 72–78.
 - [76] A. Piotrowska, J. Wierzbicka, T. Sleboda, M. Wozniak, R.C. Tuckey, A.T. Slominski, et al., Vitamin D derivatives enhance cytotoxic effects of H₂O₂ or cisplatin on human keratinocytes, *Steroids* 110 (2016) 49–61.
 - [77] A.T. Slominski, T.K. Kim, J.V. Hobarth, A.S.W. Oak, E.K.Y. Tang, E.W. Tieu, et al., Endogenously produced nonclassical vitamin D hydroxy-metabolites act as “biased” agonists on VDR and inverse agonists on RORalpha and RORgamma, *J. Steroid Biochem. Mol. Biol.* 173 (2017) 42–56.
 - [78] E.H. Sarsour, M.G. Kumar, L. Chaudhuri, A.L. Kalen, P.C. Goswami, Redox control of the cell cycle in health and disease, *Antioxidants Redox Signal.* 11 (12) (2009) 2985–3011.
 - [79] C.H. Foyer, M.H. Wilson, M.H. Wright, Redox regulation of cell proliferation: bioinformatics and redox proteomics approaches to identify redox-sensitive cell cycle regulators, *Free Radic. Biol. Med.* 122 (2018) 137–149.
 - [80] J.E. Conour, W.V. Graham, H.R. Gaskins, A combined in vitro/bioinformatic investigation of redox regulatory mechanisms governing cell cycle progression, *Physiol. Genom.* 18 (2) (2004) 196–205.
 - [81] A.R. Barr, S. Cooper, F.S. Heldt, F. Butera, H. Stoy, J. Mansfeld, et al., DNA damage during S-phase mediates the proliferation-quiescence decision in the subsequent G1 via p21 expression, *Nat. Commun.* 8 (2017) 14728.
 - [82] Q.Y. Yang, J.H. Li, Q.Y. Wang, Y. Wu, J.L. Qin, J.J. Cheng, et al., MTA1 promotes cell proliferation via DNA damage repair in epithelial ovarian cancer, *Genet. Mol. Res.* 13 (4) (2014) 10269–10278.
 - [83] A.I. Otto, L. Riou, C. Marionnet, T. Mori, A. Sarasin, T. Magnaldo, Differential behaviors toward ultraviolet A and B radiation of fibroblasts and keratinocytes from normal and DNA-repair-deficient patients, *Cancer Res.* 59 (6) (1999) 1212–1218.
 - [84] D.T. Yin, Q. Wang, L. Chen, M.Y. Liu, C. Han, Q. Yan, et al., Germline stem cell gene PIWIL2 mediates DNA repair through relaxation of chromatin, *PLoS One* 6 (11) (2011) e27154.
 - [85] L. Riou, E. Eveno, A. van Hoffen, A.A. van Zeeland, A. Sarasin, L.H. Mullenders, Differential repair of the two major UV-induced photolesions in trichothiodystrophy fibroblasts, *Cancer Res.* 64 (3) (2004) 889–894.
 - [86] M. Long, S. Tao, M. Rojo de la Vega, T. Jiang, Q. Wen, S.L. Park, et al., Nrf2-dependent suppression of azoxymethane/dextran sulfate sodium-induced colon carcinogenesis by the cinnamon-derived dietary factor cinnamaldehyde, *Cancer Prev. Res. (Phila.)* 8 (5) (2015) 444–454.
 - [87] S. Tao, M. Rojo de la Vega, H. Quijada, G.T. Wondrak, T. Wang, J.G. Garcia, et al., Bixin protects mice against ventilation-induced lung injury in an NRF2-dependent manner, *Sci. Rep.* 6 (2016) 18760.
 - [88] A. Chaiprasongsuk, T. Onkokoosong, T. Pluemsamran, S. Limsaengurai, U. Panich, Photoprotection by dietary phenolics against melanogenesis induced by UVA through Nrf2-dependent antioxidant responses, *Redox Biol.* 8 (2016) 79–90.
 - [89] S. Tao, R. Justiniano, D.D. Zhang, G.T. Wondrak, The Nrf2-inducers tanshinone I and dihydrotanshinone protect human skin cells and reconstructed human skin against solar simulated UV, *Redox Biol.* 1 (2013) 532–541.
 - [90] R. Justiniano, J.D. Williams, J. Perer, A. Hua, J. Lesson, S.L. Park, et al., The B6-vitamin pyridoxal is a sensitizer of UVA-induced genotoxic stress in human primary keratinocytes and reconstructed epidermis, *Photochem. Photobiol.* 93 (4) (2017) 990–998.
 - [91] A. Ali, M.A. Rashid, Q.Y. Huang, C.L. Lei, Influence of UV-A radiation on oxidative stress and antioxidant enzymes in *Mythimna separata* (Lepidoptera: noctuidae), *Environ. Sci. Pollut. Res. Int.* 24 (9) (2017) 8392–8398.
 - [92] R. Bisquert, S. Muniz-Calvo, J.M. Guillamon, Protective role of intracellular melatonin against oxidative stress and UV radiation in *Saccharomyces cerevisiae*,

- Front. Microbiol. 9 (2018) 318.
- [93] C. Liu, D. Vojnovic, I.E. Kochevar, U.V. Jurkunas, UV-A irradiation activates nrf2-regulated antioxidant defense and induces p53/caspase3-dependent apoptosis in corneal endothelial cells, *Investig. Ophthalmol. Vis. Sci.* 57 (4) (2016) 2319–2327.
- [94] L. Calvo-Castro, D.N. Syed, J.C. Chamcheu, F.M. Vilela, A.M. Perez, F. Vaillant, et al., Protective effect of tropical highland blackberry juice (*Rubus adenotrichos* Schltdl.) against UVB-mediated damage in human epidermal keratinocytes and in a reconstituted skin equivalent model, *Photochem. Photobiol.* 89 (5) (2013) 1199–1207.
- [95] E. Adisen, A. Gulekon, O. Erdem, A. Dursun, M.A. Gurer, The effects of calcipotriol and methylprednisolone asepionate on bcl-2, p53 and ki-67 expression in psoriasis, *J. Eur. Acad. Dermatol. Venereol.* 20 (5) (2006) 527–533.
- [96] D.A. Bubshait, D.A. Al-Dakheel, F.M. Alanii, Topical vitamin D3: a randomized controlled trial (RCT), *Clin. Nutr. ESPEN* 27 (2018) 16–19.
- [97] Z. Janjetovic, Z.P. Nahmias, S. Hanna, S.G. Jarrett, T.K. Kim, R.J. Reiter, et al., Melatonin and its metabolites ameliorate ultraviolet B-induced damage in human epidermal keratinocytes, *J. Pineal Res.* 57 (1) (2014) 90–102.
- [98] A.T. Slominski, T.K. Kim, Y. Takeda, Z. Janjetovic, A.A. Brozyna, C. Skobowiat, et al., ROR α and ROR γ are expressed in human skin and serve as receptors for endogenously produced noncalcemic 20-hydroxy- and 20,23-dihydroxyvitamin D, *FASEB J. Offic. Publ. Federation Am. Soc. Exp. Biol.* 28 (7) (2014) 2775–2789.
- [99] J. D'Orazio, S. Jarrett, A. Amaro-Ortiz, T. Scott, UV radiation and the skin, *Int. J. Mol. Sci.* 14 (6) (2013) 12222–12248.
- [100] J.F. Scott, L.M. Das, S. Ahsanuddin, Y. Qiu, A.M. Binko, Z.P. Traylor, et al., Oral vitamin D rapidly attenuates inflammation from sunburn: an interventional study, *J. Investig. Dermatol.* 137 (10) (2017) 2078–2086.
- [101] J.F. Scott, K.Q. Lu, Vitamin D as a therapeutic option for sunburn: clinical and biologic implications, *DNA Cell Biol.* 36 (11) (2017) 879–882.
- [102] A. Slominski, D.J. Tobin, S. Shibahara, J. Wortsman, Melanin pigmentation in mammalian skin and its hormonal regulation, *Physiol. Rev.* 84 (4) (2004) 1155–1228.
- [103] A.T. Slominski, Z. Janjetovic, T.K. Kim, A.C. Wright, L.N. Grese, S.J. Riney, et al., Novel vitamin D hydroxyderivatives inhibit melanoma growth and show differential effects on normal melanocytes, *Anticancer Res.* 32 (9) (2012) 3733–3742.
- [104] K. Abeyama, W. Eng, J.V. Jester, A.A. Vink, D. Edelbaum, C.J. Cockerell, et al., A role for NF-kappaB-dependent gene transactivation in sunburn, *J. Clin. Investig.* 105 (12) (2000) 1751–1759.
- [105] I. Bellezza, I. Giambanco, A. Minelli, R. Donato, Nrf2-Keap 1 signaling in oxidative and reductive stress, *Biochim. Biophys. Acta Mol. Cell Res.* 1865 (5) (2018) 721–733.
- [106] U. Wasik, M. Milkiewicz, A. Kempinska-Podhorodecka, P. Milkiewicz, Protection against oxidative stress mediated by the Nrf2/Keap 1 axis is impaired in Primary Biliary Cholangitis, *Sci. Rep.* 7 (2017) 44769.
- [107] R.C. Tuckey, Z. Janjetovic, W. Li, M.N. Nguyen, M.A. Zmijewski, J. Zjawiony, et al., Metabolism of 1 α -hydroxyvitamin D3 by cytochrome P450 $_{\text{scc}}$ to biologically active 1 α ,20-dihydroxyvitamin D3, *J. Steroid Biochem. Mol. Biol.* 112 (4–5) (2008) 213–219.
- [108] Z. Lin, H. Chen, A.Y. Belorusova, J.C. Bollinger, E.K.Y. Tang, Z. Janjetovic, et al., 1 α ,20S-Dihydroxyvitamin D3 interacts with vitamin D receptor: crystal structure and route of chemical synthesis, *Sci. Rep.* 7 (1) (2017) 10193.
- [109] Z. Lin, S.R. Marepally, D. Ma, T.K. Kim, A.S. Oak, L.K. Myers, et al., Synthesis and biological evaluation of vitamin D3 metabolite 20S,23S-dihydroxyvitamin D3 and its 23R epimer, *J. Med. Chem.* 59 (10) (2016) 5102–5108.
- [110] E.K. Tang, W. Li, Z. Janjetovic, M.N. Nguyen, Z. Wang, A. Slominski, et al., Purified mouse CYP27B1 can hydroxylate 20,23-dihydroxyvitamin D3, producing 1 α ,20,23-trihydroxyvitamin D3, which has altered biological activity, *Drug Metab. Dispos.* 38 (9) (2010) 1553–1559.